ORGANIZATION OF BIOMOLECULES IN A 3-DIMENSIONAL SPACE

by

Sameer Sajja

A thesis submitted to the faculty of
The University of North Carolina at Charlotte
in partial fulfillment of the requirements
for the degree of Master of Science in
Chemistry

Charlotte

2019

Approved by:

_____
Dr. Kirill Afonin

_____
Dr. Caryn Striplin

_____
Dr. Joanna Krueger

_____
Dr. Yuri Nesmelov

ABSTRACT

SAMEER SAJJA. Organization of Biomolecules in a 3-Dimensional Space
(Under the direction of DR. KIRILL A. AFONIN)

The human body operates using various stimuli-responsive mechanisms, dictating biological activity via reaction to external cues. Hydrogels are networked hydrophilic polymeric materials that offer the potential to recreate aqueous environments with controlled organization of biomolecules for research purposes and potential therapeutic use. The unique, programmable structure of hydrogels exhibit similar physicochemical properties to those of living tissues while also introducing component-mediated biocompatibility. The design of stimuli-responsive biocompatible hydrogels would further allow for controllable mechanical and functional properties tuned by changes in environmental factors. This study investigates individual biomolecular components needed to potentially engineer biocompatible and stimuli-responsive hydrogels. By utilizing programmable biomolecules such as nucleic acids (DNA and RNA) and proteins (actin), we can achieve high component biocompatibility while progressing toward understanding the designing principles for stimuli-responsive, functional hydrogels.

ACKNOWLEDGEMENTS

Research reported in this thesis regarding the dynamic behavior of RNA hexameric rings and their physicochemical and immunological property characterization as described in the related publication (*Langmuir*, 34(49): 15099-15108, 2018. PMID: 29669419) was supported by the National Institute Of General Medical Sciences of the National Institutes of Health under Award Number R01GM120487 (to Kirill A. Afonin). The content is solely the responsibility of the authors and does not necessarily represent the official views of the National Institutes of Health. This project has been funded in part with federal funds from the Frederick National Laboratory for Cancer Research, National Institutes of Health, under contract HHSN261200800001E (Wojciech K. Kasprzak, Mathias Viard, Ankit Shah, and Marina A. Dobrovolskaia). This research was supported in part by the Intramural Research Program of the NIH, National Cancer Institute, Center for Cancer Research (Bruce A. Shapiro). The content of this publication does not necessarily reflect the views or policies of the Department of Health and Human Services, nor does mention of trade names, commercial products, or organizations imply endorsement by the U.S. Government. This study used computational resources and support of the National Cancer Institute's Advanced Biomedical Computing Center. We are grateful to Mr. Barry Neun for the excellent technical assistance and thank Dr. Emil Khisamutdinov and Ms. Victoria Goldsworthy of Ball State University for help with DLS experiments. Research reported herein regarding the fluorescent split RNA aptamer "Broccoli" and related publication in the Journal of Chemical Education was done with the help of undergraduate lab members Dylan Dang, Jared Dahl, Allison Tran, Lauren Lee, Beamlak Worku, and Steven Woods for testing all protocols during development, Melina Richardson for testing protocols and assisting in illustrations, and students enrolled in the CHEM 4090/5090: Nanobiochemistry course at the University of 325 North Carolina at Charlotte. Actin was provided by Dr. Yuri Nesmelov, and AFM images were taken by Alexander Lushnikov at the nanoimaging facility at the University of Nebraska.

TABLE OF CONTENTS

LIST OF FIGURES vii

LIST OF ABBREVIATIONS viii

CHAPTER 1: INTRODUCTION TO NANOMATERIALS AND HYDROGELS 1

1.1 The field of nanotechnology 1

1.2 Hydrogels 2

CHAPTER 2: PROJECT OVERVIEW AND OBJECTIVES 9

CHAPTER 3: PROTIENS 10

3.1 Proteins – An overview of actin and other proteins 10

CHAPTER 4: NUCLEIC ACIDS 13

4.1 Nucleic Acids – An Overview 13

4.2 Development of Nucleic Acid Technology 13

4.3 Nucleic Acid Structures and Motifs - Development 15

4.4 Development of Hexameric NA Nanoparticle 17

4.5 Experimental Development of Hexameric Nanoparticle 18

4.6 Our modification to the Hexameric Nanoparticle – Introduction of 6nt Gaps 19

CHAPTER 5: BIOCONJUGATION 28

5.1 Bioconjugation types 28

5.2 Covalent Bioconjugation Techniques 28

5.3 Actin Bioconjugation - Covalent Approach to Crosslinking 29

5.4 Cysteine Bioconjugation 29

5.5 Incorporation of biomolecules into a hydrogel 30

5.6 Characterization of DNA-Actin Bioconjugation 32

5.7 DNA-Actin Bioconjugation Conclusion 32

CHAPTER 6 - VISUALIZATION OF HYDROGEL FORMATION VIA “BROCCOLI” RNA APTAMER 33

6.1 Visualization techniques/Significance 33

6.2 RNA Visualization techniques/Significance 34

6.3 Development of RNA Aptamer “Broccoli” 34

CHAPTER 7: CONCLUSION 41

REFERENCES 43

APPENDIX: SEQUENCES USED AND ACTIN EXPERIMENTAL PROCEDURES 54

LIST OF FIGURES

FIGURE 1: Conceptual Schematic of proposed hydrogel 9

FIGURE 2: Diagram of actin 11

FIGURE 3: Streptavidin and Biotin structure and binding 12

FIGURE 4: DNA/RNA Base Pairing Diagram 13

FIGURE 5: Basic structure of hexameric RNA nanoparticle 19

FIGURE 6: Characterization of the gapped RNA hexameric nanoparticle 21

FIGURE 7: Ring deformation and AFM images of hexameric nanoparticle 23

FIGURE 8: Computational algorithmic deformation analysis of hexameric nanoparticle 25

FIGURE 9: Application of RNA nanoring as crosslinker for a hydrogel 26

FIGURE 10: Diagram of G to F-actin conformational change 29

FIGURE 11: Cysteine and Maleimide Reaction 30

FIGURE 12: Reagents used in Nucleic Acid Bioconjugation 30

FIGURE 13: Schematic of DNA-actin Hydrogel with maleimide oligo 31

FIGURE 14: Actin Hydrogel Characterization 32

FIGURE 15: Broccoli aptamer structure and schematic 37

FIGURE 16: Visualization of Broccoli fluorescence 39

FIGURE 17: Incorporation of Broc+Coli aptamer in hydrogel 40

LIST OF ABBREVIATIONS

AFM	Atomic Force Microscopy
DF	Deformation Factor
DFHBI-1T	(5Z)-5-[(3,5-Difluoro-4-hydroxyphenyl)methylene]-3,5-dihydro-2-methyl-3-(2,2,2-trifluoroethyl)-4H-imidazol-4-one
DLS	Dynamic Light Scattering
DNA	Deoxyribonucleic Acid
dsRNA	Double stranded RNA
ECM	Extracellular matrix
EtBr	Ethidium Bromide
F-actin	Fibrous actin
FRET	Förster resonance energy transfer
G-actin	Globular actin
GFP	Green Fluorescent Protein
HA	Hyaluronic acid
HABA	(4'-hydroxyazobenzene-2-carboxylic acid)
HBI	4-(p-hydroxybenzylidene)imidazolidin-5-one
hSAFs	Hydrogelating self-assembling fibers
IFN	Interferon
MS2-GFP	Muashi System 2 – Green Fluorescent Protein
NANP	Nucleic Acid Nanoparticle
NP	Nanoparticle
PAGE	Poly Acrylamide Gel Electrophoresis
pHEMA	Poly(2-hydroxyethyl) methacrylate
PVA	Polyvinyl alcohol
RNA	Ribonucleic Acid

RNAi	RNA interference
SELEX	Systematic evolution of ligands by exponential enrichment
siRNA	Small interfering RNA

CHAPTER 1: INTRODUCTION TO NANOMATERIALS AND HYDROGELS

1.1 The field of nanotechnology has been rapidly developing in the last decades with advancements towards therapeutic and diagnostic applications.[1] Current applications of therapeutic nanotechnology includes the development of biomedical nanodevices, three-dimensional (3D) scaffolds for tissue engineering and material organization, and drug delivery platforms, just to name a few.[2]

The construction of nanomaterials – which are defined as the controlled organization of matter on an atomic, molecular, or supramolecular scale - has been achieved with inorganic ligands and metal complexes as well as with biomolecules among which are proteins, lipids, and nucleic acids.[3] Utilization of biomolecules for the synthesis of nanomaterials offers a myriad of benefits when compared to purely inorganic or synthetic materials, as the use of inorganic materials to produce nanoparticles (NPs) for diagnostics and treatment is often problematic due to several factors, including toxicity of starting components, industrial contamination, and the potential for uncontrolled bioaccumulation.[1a, 4]

Biological systems are composed of highly ordered and organized 3D biostructures. This organization promotes the precise interaction of the functional parts and facilitates the necessary biological functions needed for life to occur. To promote the understanding of the structure-activity relationship of biological systems, each respective part as well as the general biochemical environment in which these various parts interact can be individually modeled and investigated. One way to do this is to create an artificial matrix with deliberately embedded biomolecules to mimic the fragments of naturally occurring structures. Therefore, the controlled and predictable organization of biomolecules in 3D space became an important focus in the elucidation of the various systems that result from this biological architecture. Hydrogels, hydrophilic polymeric materials that maintain a distinct three-dimensional organization, are highly promising candidates for the study of the aqueous intracellular structure of cells, and have potential biomedical use.[5] Due

to their water content, porosity, and softness, hydrogels can effectively simulate natural living tissue and extracellular matrix (ECM).[5a]

1.2 - Hydrogel structures are a naturally occurring part of endogenous biological systems. A variety of natural hydrogel forming compounds such as fibrin, hyaluronic acid, alginate, *etc* have been investigated for their role in the cellular organization of biological 3D networks.[6] Biological gels such as mucus and the ECM each have unique characteristics that enable a precise biological function.[7] The ECM, an interlocking mesh of fibrous proteins and glycosaminoglycans, enables cellular communication, differentiation, migration, structural support, and acts as a temporary storage for cellular growth factors.[8] Overall, the ECM provides a wide array of bioactive functionalities that have the potential to be incorporated into programmable hydrogel scaffolds in order to enable mimicry of the aforementioned biological mechanisms.[9] By imitating this natural environment, it should become possible to direct intrinsic natural function and processes toward a pre-programmed biological function.

From the initial foray into hydrogel research beginning in 1860, many advancements have been made, transforming hydrogels from their nascent early design to the complex gels used in modern applications.[10] The term 'hydrogel' first appeared in the literature in 1896, coined by Bemmelen et al. who used iron oxide to construct the first hydrogel structures.[11] The first synthetic hydrogel was not explored until later in 1954 by Wichterle et al.[12] The initial studies done by Wichterle et al. were directed towards biocompatibility of synthetic plastics for biomedical application, leading to the synthesis of Poly(2-hydroxyethyl) methacrylate (pHEMA) by 1960 for use in synthetic contact lenses. Hydrogel research developed rapidly both commercially and academically, with Kleiner et al. receiving a patent for their novel synthesis of polysiloxane hydrogels and with the landmark developments of Peppas et al. in the field of drug release and synthetic biocompatible hydrogels- each with potential for use in biomedical applications.[13]

The next important development in hydrogel research can be credited to the 1974 work of Peppas et al. which utilized polyvinyl alcohol (PVA) as a monomer crosslinked via γ-radiation at

different incident angles to modulate crosslinking ratios.[13b] This discovery and consequent synthesis played an integral role in the future development of biocompatible hydrogel materials; the ability to modulate the properties of the gel enables tunability of its mechanical characteristics and functionality. Subsequent work conducted by Langer et al. in 1976 catalyzed further research on drug release behavior characteristics in different hydrogel systems.[14] Heparin functionalized hydrogels, a key secondary-stage application of this original work, were also developed by Peppas et al. in 1977 as one of the first examples of a PVA hydrogel for biomedical applications.[15] By 1981, hydrogels were adapted to a wide variety of pharmaceutical applications in various stages of research from *in vitro* experimentation to commercially marketed hydrogels. The synthetic polymers were seminally used in a biomedical application by Vacanti et al. in 1988 for selective transplantation of cells utilizing similar biocompatible/bioabsorbable synthetic hydrogel matrices.[16] Peppas and Langer later developed and applied a set of design principles to hydrogel research and set the foundation for the next decade of discoveries.[17]

At that time, the controlled release of a therapeutic payload was a main focus of hydrogel research.[17] By 1990, a few hydrogel-based drug release therapeutic platforms were developed in the fields of ophthalmology and contraception.[17] Building on the discoveries of the previous decade of research, commercially available synthetic hydrogels Occusert and Progestasert were used as eye drops and for long-term progesterone dosing, respectivelly.[17-18]

Research focus on controlled drug release, along with the well-characterized monomers in use for hydrogel synthesis, eventually shifted towards environmentally responsive hydrogel systems.[19] In 1991, Peppas et al. reviewed the current state of responsive systems, focused on pH, ionic strength, and temperature dependency with targeted application.[20] pH responsive gels were demonstrated to be useful in achieving a specific drug release within the intestines with pH ~ 6.5 but not in the stomach at pH~1.5.[19] Later, the focus of hydrogel research shifted again, and until 2000, the hydrogel development largely concentrated on rationally designed systems to achieve improved physical and mechanical characteristics.[21]

A notable discovery was that of Whitesides et al. in the field of molecular self-assembly, which was the spontaneous association of molecules under equilibrium conditions into stable, well-defined aggregates that are not covalently bound.[22] Similar to the work of Peppas and Langer, Whitesides' work focused on creating an organized structure of molecules that could be used in biomedical applications.[22] While his work was mostly focused on chemical synthesis and lithography, Zhang et al. followed Whitesides' work in 1993 with the identification of a naturally occurring peptide in yeast that in the presence of salt can self-assembled into a macroscopic membrane-like structures.[23] This research was followed by the work of Tirrell et al. in 1998, where researchers used recombinant DNA technology to 'express' custom peptide sequences that organized themselves into a hydrogel structure and possessed the ability to be responsive.[1b] Tirrell's work addressed the problem of the two seemingly contradictory behaviors that gel formation demanded: that interchain interactions linking different components of a gel must be both strong enough to act as gel junction points without breaking, yet be porous to allow solubilization and swelling rather than precipitation of the structure out of the solution.[1b] The gel design approach addressed these concerns through the creation of multidomain "triblock" of artificial proteins, within which the interchain binding and solvent retention functions are engineered independently.[1b] Their findings of sequence-dependent structure demonstrated the effect of hydration on each motif inherent in the co-block peptide construct of the hydrogel.[1b] In a review of the state of hydrogel research, Peppas identified that hydrogels presented a significant opportunity in the pharmaceutical sciences due to the discoveries made in advanced drug delivery formulations over the previous 20 years.[21] Rather than releasing the payload at a characteristic rate, hydrogel therapeutics delivered drugs more efficiently through location based application and enzymatic, hydrolytic, or environmental stimuli.[21, 24] Prior to this, constituents of biological origins, such as phospholipids, amino acids, *etc*, were overlooked as traditional building materials, however, rapid developments in biotechnology rekindled their use in the field of biomaterials engineering.[1b, 25]

Both molecular self-assembly and hydrogel research goals centered around the potential creation of synthetic tissue with natural tissue behavior.[21] Supramolecular self-assembly and rational hydrogel monomer design were tied together by the work of Stupp et al. in the early 2000s.[26] Molecular self-assembly and organization was later expanded by Hwang et al. in which they reported on the synthesis and characterization of self-assembling biomaterials with deliberate molecular features designed to interact with cells and act as scaffolds for tissue engineering.[26a] Self-assembling biomaterials would be particularly useful in medicine, as the formation of targeted structures could be programmed to occur when the gel comes in contact with tissues.[26b] Additionally, the control over 3D structure can address the spatial organization of bioactive ligands to directly impact the behavior of cells through proximal interaction.[26b] Such control could impact a material's ability to promote cell division, differentiation, and synthesis of extracellular matrix for tissue engineering.[25, 27] In a 2002 review on emerging biological materials, Zhang et al. identified type I, ''molecular legos'' that form hydrogel scaffolds for tissue engineering.[28] These type I structures contain two distinct surfaces: one hydrophilic and the other hydrophobic and can form beta-sheet structures in aqueous solution.[28] The basis of a self-assembling peptide hydrogel design was to use monomers that can undergo spontaneous stepwise interactions and assemblies via the formation of numerous weak noncovalent chemical bonds as defined by Pauling et al. in his work on non-covalent binding.[28-29] A 2004 inquiry by Pochan et al. into the folding and self-assembly of beta-hairpin peptides into rigid hydrogels, demonstrated that the physical characteristics of the gel itself depended on the salt concentration of the environment as well as the ionic interactions with the hydrophilic and hydrophobic regions of the peptide sequences used.[30] Building upon this exploration, the first examples of rationally designed and fully characterized self-assembling hydrogels synthesized by Woolson et al. emerged utilizing standard linear peptides with purely alpha-helical structures, called hydrogelating self-assembling fibers (hSAFs).[31] The peptide sequences of these hSAFs can be engineered to alter the underlying mechanism of gelation and, by consequence, the hydrogel properties themselves via environmentally responsive systems.[31]

Beginning in 2010, engineered synthetic hydrogels started to be explored as ECM mimics.[32] Advances in the design of artificial matrices aimed in development of hydrogels from playing the role of simple supporting scaffolds to adopting the qualities of a dynamic biomaterials.[33] Ideally, these artificial matrices should support cell growth and maintenance and possess appropriate mechanical, chemical, and biological characteristics mimicking the native ECM.[9, 32-33] The increased exploration of ECM enabled understanding of how to utilize the core conceptual components of hydrogels for advanced biomedical applications that require embedded functionality, stimuli-responsiveness, and dynamic behavior that also maintain stability and biocompatibility.[9, 32-34]

In recent years, protein chemistry gained increased utility in the development of hydrogels, due to their numerous inherent advantages including stability, versatility, and potentially tunable folding and programmable interactions.[35] Peptides and proteins may be conjugated to hydrogel components or provide structural integrity to a gel via self-assembly or aggregation.[26b, 28, 31, 34 35] The small globular protein lysozyme, present in the white of a hen's egg, had been investigated by Yan et al. as a biomaterial candidate due to the organized actin filaments in the form of stress fibers formed within the fibroblasts.[36] This demonstrated that lysozyme gels could potentially be a viable support for the interstitial cells and established their potential as scaffolds for tissue engineering.

Current, advancements in the field include biomolecule-embedded gels for dressing wounds, and increased development of artificial tissues, with the main impetus being the synthesis of biomedical gels for implantable and external use.[37] Actin, one of the most common proteins in the eukaryotic cytoskeleton, plays a vital role in biological scaffolding. A cell's ability to form microfilaments, in response to external or internal stimuli, provides the framework that allows it to remodel itself as needed. Therefore, actin inherently plays an important role in embryogenesis, wound healing, and controlling the invasive nature of cancerous cells.[38] Actin exists in the cell in two conformations, globular actin (G-actin) and fibrous actin (F-actin). G-actin changes its conformation to F-actin to form the fibers. The F-actin cytoskeleton rarely exist as individual

fibrous structures in the cell but appear as hydrogel-like networks where actin binds proteins, such as espin, fascin, scruin, filamin, *etc*. that behave as physical cross-linkers, linking the different F-actin fibers together.[39] Several types of F-actin networks classified as weakly crosslinked networks, composite networks, bundle networks, and bundled cluster networks, were prepared using this approach.[39-40] Synthesis of different actin-based gel structures allowed for an understanding of how the actin cytoskeleton behaves inside a cell. Furthermore, actin itself has the potential to act as a suitable hydrogel component as it offers the benefits of a peptide-based construct outlined above. Similarly, structural and functional nucleic acids can be used as a bioactive hydrogel component given their ubiquitous nature in eukaryotic systems and their variety of intrinsic functions. By exploring different types of hydrogel monomers and crosslinkers, past hydrogel principles can be applied to new components or component combinations to create novel hydrogels for biochemical and biomedical use.

From the foundations of hydrogel research, a few key characteristics become apparent for practical use: embedded functionality, stimuli-responsive behavior, and biocompatibility. The aqueous scaffolded nature of hydrogels enables programmable bioactivity *via* embedded therapeutic payloads. Used for both diagnostic and therapeutic applications, embedded functional biomolecules, such as, for example, nucleic acids, would allow for finely tunable functions *via* non-reactive biorthogonal hydrogel scaffolding and selective bioactive payloads. Stimuli-responsive hydrogel-mediated drug delivery, on the other hand, involves the use of polymer systems that are designed to respond to physicochemical and physiological stimuli. These polymers are unique in their structural response to environmental changes, with the ability to revert to their native state once stimuli is removed.[34, 41] These structural changes can be utilized for conditionally activated hydrogel systems in response to changes such as heating, pH, light, and embedded chemicals in order to facilitate a programmed response for use in biomedical therapeutics. [6b, 42] A responsive gel system is especially impactful as it allows for a dosage system that would only apply in the right

situation rather than a non-regulated broad-spectrum diffusive application that impacts the host biologically.

CHAPTER 2: PROJECT OVERVIEW AND OBJECTIVES

The overall goal of this project was to synthesize a proof-of-concept hydrogel, utilizing various classes of biomolecules (nucleic acids and proteins) to create a foundation for future hydrogel studies. Actin (Figure 1-1), a ubiquitous polymerizing eukaryotic protein, serves as an excellent component for the construction of a biomaterial hydrogel due to its inherent characteristics of self-assembly and biocompatibility. Various classes of biomolecular crosslinks, such as RNA and DNA molecules, can be employed to act as both functional and structural units. For the proposed hydrogel design (Figure 1) we aimed to complete the following steps: (i) to develop programmable RNA nanoassemblies which have tunable flexibility and functionalization to be used as dynamic crosslinks; (ii) to explore the design of a fluorescent RNA reporters to be used for real-time tracking of the hydrogel formation; and (iii) to develop a protocol of bioconjugation between actin fibers and chemically modified nucleic acids.

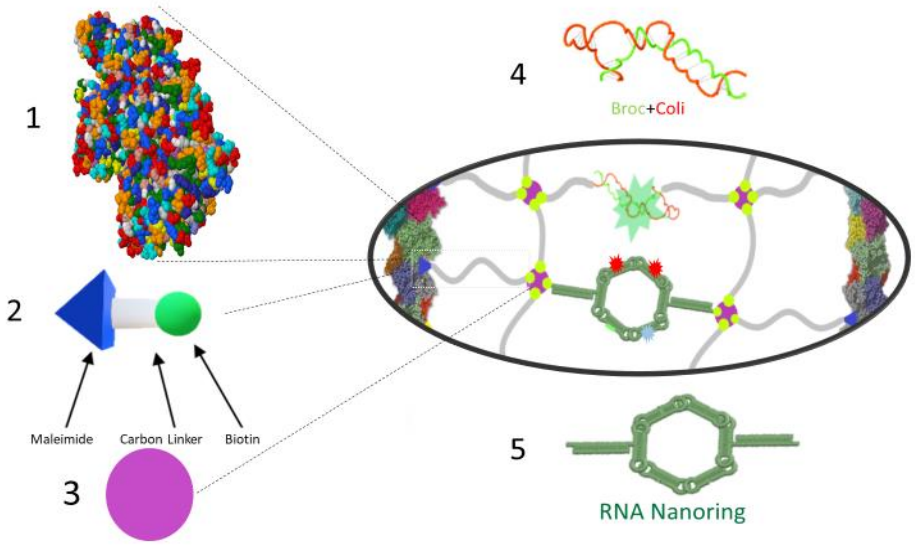

Figure 1 Conceptual description of the proposed hydrogel with the 1) Actin backbone linked via a maleimide-biotin linker molecule/oligonucleotide to a central 3) Streptavidin hub which links the 4) RNA aptamer and 5) functionalized hexameric nanoring scaffold

CHAPTER 3. PROTIENS

3.1 - Proteins, large biomolecules consisting of chains of amino acid residues, perform a vast array of functions in nature, making them promising candidates for nanomaterial applications.[1b, 3c, 35] The specific 3D organization of proteins – achieved through the protein's unique amino acid sequence – determines their biological activity.[43] Polymerizing proteins therefore are anticipated to serve as good biomaterial hydrogel components due to their natural ability to serve as a cellular scaffold. One promising candidate that we consider for hydrogel formation is actin, is a large component of the cytoskeleton and has a structure dependent function that enables conditional fiber formation in the cell.[38a, 44] Shown in Figure 2 is a diagram of an actin monomer as a part of a larger actin fiber, as well as the specific residue interactions that hold the fiber together. Cells assemble F-actin into various structures ranging from dilute networks to bundles of closely packed F-actin filaments.[38a] This biopolymer network is crucial for processes that require variations in the cytoskeleton, such as cell migration, division and intracellular transport.[38, 45] To construct dynamic F-actin assemblies with specific morphologies and mechanical properties, cells make use of actin-binding molecules. These molecules bind to actin and crosslink F-actin fibers, changing the organization of the fibers in the cytoskeleton as needed.[38a, 45] The cytoskeleton therefore must combine structural integrity and mechanical stability with the ability to undergo fast and efficient network reorganization and dynamic restructuring.[44] Due to the complexity inherent to actin, monitoring actin behavior has been difficult *in vivo*, and well-defined *in vitro* model systems demonstrated effective value in uncovering the physical principles that determine the structural polymorphism (shape changing ability) in cytoskeletal networks.[46] By synthesizing an actin hydrogel with increasing complexity, the influence of biochemical and physical contributions to both the network mechanics and organization can be elucidated and potentially utilized for a therapeutic hydrogel platform as explored by Osada et al. in 2011.[47]

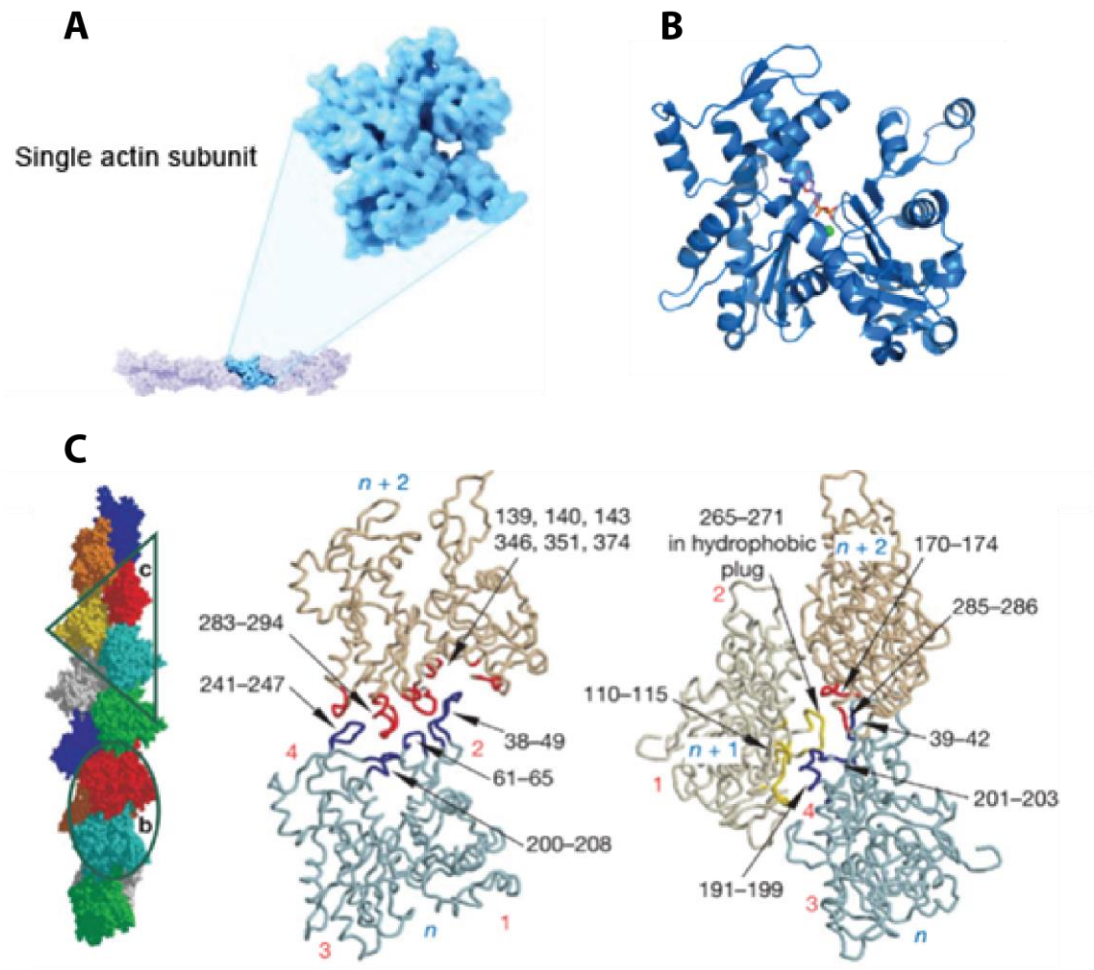

Figure 2. 2A. Diagram of a single actin subunit. 2B. Ribbon Diagram of G-Actin. 2c. (left) F-Actin Structure with monomers identified, (middle) Intramolecular residue interactions in F-Actin, (right) Inter-Actin residue interactions. Images from [44]

Proteins, from being used as a hydrogel backbone, can also be used as crosslinking avenues to hold together different components of the gel itself, namely the biotin-streptavidin interaction found in nature.[38a, 45] Streptavidin, a 66.8 kDa molecule, has 4 binding sites for Biotin (Vitamin H), with one of the strongest well-demonstrated non-covalent interactions in nature (K_D=10^-15). [48] The molecular structure of biotin and its binding to streptavidin are shown in Figure 3.

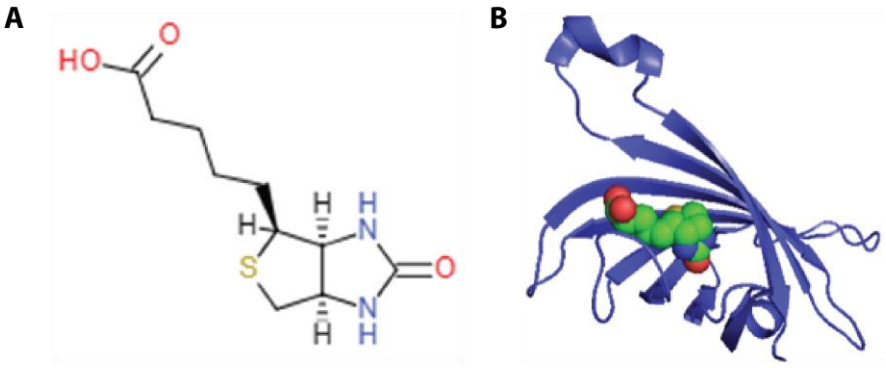

Figure 3. 3A. Biotin structure. 3B. Biotin bound to Streptavidin binding site[48]

Streptavidin maintains stability and biotin binding affinity in physiological conditions (pH ~7), making it a suitable candidate for a protein crosslinker and as a functional handle for an RNA payload.[48] Biotin is an endogenous molecule that binds tightly to streptavidin. Due to its small size (244 Da) and well- established history as a bioconjugation tool, it serves as a suitable candidate for a crosslinker component.[48] RNA linked via streptavidin as a potential crosslinking component has been demonstrated and reviewed by our lab in the work of myself and Roark et al. and could be achieved with a biotin functionalized RNA strands attached to a nanoparticle scaffold or RNA aptamer.[49]

CHAPTER 4: NUCLEIC ACIDS AS CROSSLINKERS AND FUNCTIONAL UNITS

4.1 - Nucleic acids (DNA and RNA) have been explored as promising candidates for nanomaterial synthesis due to their unique physical, chemical, and biological properties.[50] The base pairing (Shown in Figure 4) and resulting secondary structure give nucleic acids a sequence dependent structure. The potential for synthesis of a DNA based hydrogel has only recently been explored, having applications in a variety of areas including but not limited to biosensing,[51] controlled drug release,[52] cell adhesion,[53] and cancer therapy.[54] Each of these applications shows promise in the controlled construction of nucleic acid-hybrid materials with broad range of biomedical applications.

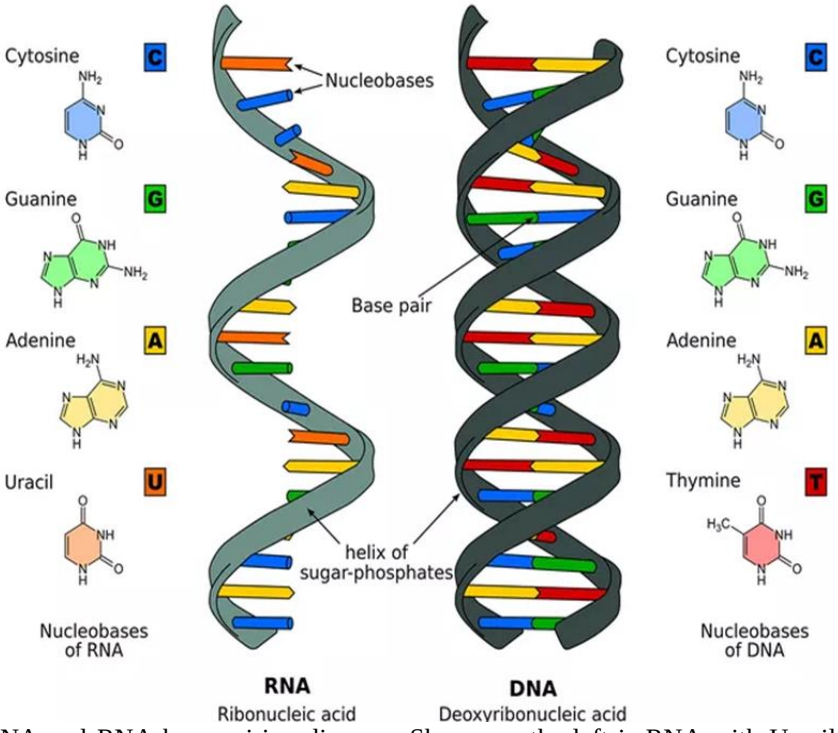

Figure 4. DNA and RNA base pairing diagram. Shown on the left is RNA with Uracil replacing the Thymine in DNA. (Image provided by Wikimedia Commons)

4.2 - In 1971, Nadrian Seeman pioneered the field of DNA nanotechnology with his initial work regarding conformational studies of nucleic acids.[55] His research centered around the design principles of utilizing the spatial periodic network nature of DNA to orient biomolecules for 3D

diffraction analysis.[56] The simple ligation of DNA strands had already been previously explored by genetic engineers in the synthesis of linear recombinant DNA.[57] In his work, Seeman used the complementary nature of DNA base pairing along with its predictable secondary structure due to canonical Watson-Crick base pairing to create numerous deliberate DNA structures.[58] Holliday junctions, structures found in biological intermediates in genetic recombination, are examples of reciprocal exchange, or the crossover of two adjacent strands of DNA via canonical base pairing.[59] Other examples of DNA motifs include panaremic crossover cohesion, edge sharing, and lateral cohesion[60] raised the possibility of rigid molecular building blocks for the combinatorial construction of complex nanostructures.[58] Another powerful technique called “DNA origami” was developed a decade ago by Paul Rothemund.[61] This approach used a single-stranded DNA scaffold with many short oligonucleotide 'staple’ strands to generate different shapes made entirely of DNA.[61] Once mixed one-pot, the staple and scaffold strands self-assemble as a result of sequence dependent interactions, thus enabling the construction of larger programmable DNA nanostructures with defined shapes. DNA origami was then expanded from its original scope regarding the design of 2D structures to the design of increasingly complex 3D structures.[62] Although DNA has demonstrated the potential to act as a suitable scaffold for various nanostructures, it lacks some of the advantages offered by unique structural and functional properties only characteristic to RNA.[63] RNA’s advantages include increased thermal stability due to its unique base stacking properties and the C3’-endo conformation of the sugar as well as its ability to form noncanonical base pairing.[63] These advantages lead to the possibility of a larger variety of naturally occurring structural motifs which can be used as building blocks for other designed structures.[64]

4.3 - RNA, first characterized as a messaging component of transcription, was functionally defined in the middle of last century.[65] However, it was not until about two decades later, with the discoveries made by Tom Cech and Sidney Altman regarding the self-splicing of an RNA ribosomal precursor, that RNA research started gaining traction.[66] By uncovering the catalytic potential of RNA, it paved the way for the discovery of a plethora of RNA's other multitasking functions. Overall, natural catalytic RNAs operate on a hierarchical basis with primary sequence determining secondary structure, and secondary structure promoting tertiary interactions between separate structural motif.[67] In 1975, Paul Sigler discovered that secondary structure is sequence dependent due to hydrogen bonds being formed between ribose sugar side chains rather than backbone atoms.[68] This, in turn enables the elucidation of the secondary structure of RNA molecules through phylogenetic sequence comparison. In the early 2000s, Jaeger et al. proposed that different non-canonical RNA interaction motifs can be reorganized to promote the formation of artificial RNA nanostructures.[69] Coined 'RNA tectonics', it centered around similar design principles of using different RNA architectural motifs identified in nature as tools to further develop an understanding of the underlying logical rules that dictate RNA behavior.[67a, 70] Identification and characterization of different structural motifs has enabled RNA researchers to create a toolkit for the extensive development of naturally derived RNA nanoparticles for therapeutic use.[67a, 70] Various structural motifs have been used in the design of artificial RNA building blocks. One of the first examples of identifying natural RNA motifs to create deliberate nanostructure building blocks for therapeutic RNA nanotechnology was done by Peixuan Guo's group with their identification of a stable three-way junction motif (3WJ) in the packaging RNA of the bacteriophage ϕ29 dsDNA.[71] This 3-way junction motif building block was later used as an integral structural component for the creation of various RNA shaped nanoparticles, such as a triangle, square, and pentagon.[72] Similarly, in the early work by Eric Westhof, Neocles Leontis, and Luc Jaeger used the naturally occurring tetraloop structure of the P4-P6 domain of the *Tetrahymena thermophila* ribozyme to mediate deliberate, high affinity RNA-RNA interactions between RNA constructs.[67a, 70] Yaroslava Yingling

and Bruce Shapiro took this utilization of different RNA structural motifs a step further with their development of a computational ruleset for the self-assembly of an all RNA nanoparticle.[73] They summarized this with a general approach; to first take known RNA structures and divide them up into their respective building blocks and to then recreate each single stranded and looped region to achieve intended self-assembly of the artificial RNA structure via non-covalent tertiary interactions of these motifs.[73]

It is now appreciated that RNA allows for formation of 12 geometric families of base pairing which facilitate further formation of diverse RNA 3D structures with defined biological functions.[64, 69] The folding and assembly of distinct and reproducible 3D RNA structures, that define their function, are dictated by a diverse number of structural and long-range interacting motifs[70] compacting together.[63b] RNA machinery follows a general modular pattern observed from characterization of individual motifs and natural functional RNAs with ribozymes and spliceosomes being examples of key components of complex cellular network that follow this pattern.[74, 75, 76] RNA uses a variety of interstrand (between RNA strands) and intrastrand (within a RNA strand) forming structural and long-range interacting motifs such k-turns, C-loops, paranemic motifs, loop-receptor, loop-loop interactions, and pseudoknots just to name a few.[77] The different modular components of RNA can be further divided into two classes, functional units and aforementioned structural units. Functional units, or RNA structures that have intrinsic chemical or biological activity, include ribozymes, riboswitches, aptamers, short interfering RNA, micro RNA (miRNA), *etc*.[78] RNA functional units, identified in nature, are used as attachments onto RNA scaffolds or carriers. SiRNAs and miRNAs, for example, represent a class of double-stranded RNA approximately 20-25 base pairs in length which operates within the RNA interference (RNAi) pathway by interfering with the expression of specific genes.[79]

The overall strategies for RNA nanodesign, or the design and synthesis of different RNA nanostructures amenable to functionalization for therapeutic use follows two main approaches. The first is utilization of existing prefolded RNA structural motifs, relying of on correct intramolecular

hydrogen bonding, as building blocks for RNA assemblies *via* intermolecular interactions. This approach involves using preexisting natural structures and underlying rules of RNA folding to connect each individual motif. The second approach involves the utilization of relatively short single-stranded RNAs designed to only form intermolecular interactions with cognate partners.[80] Various dynamic molecular simulation programs, such as Assisted Model Building with Energy Refinement (AMBER), Avogadro, Discovery Studio, and Ascalaph Designer, to name a few, can be carefully tuned via program parameter inputs for precise structural optimization of the RNA building blocks and final nanostructures.[81] The use of MD simulations adds a benefit of being relatively inexpensive and fast way to create different proposed structural designs and assess their predicted properties.[73] Nucleic acid nanostructures created following these approaches - such as nanoparticle polygons,[82] conditionally activated RNA devices,[83] and nucleic acid hydrogels[84] - have been developed and studied for their potential use as therapeutics or bioanalytical tools with precise function in a biological environment.

The method used for the design of the hexameric RNA nanorings a versatile RNA nanoscaffold used in this project, follows the approach where different known structural motifs, in this case RNAI/II inverse kissing complexes (kissing loops), would be placed in spatial proximity in a modeling software, and then linked together by fitting helical strands of RNA to create structures. These theoretical structures would undergo computational analysis to achieve sequence optimization and then experimentally characterized. Functionalization can then be achieved simply by elongation of the 5’ or 3’ terminal ends with different functional units attached directly to RNA starnds.[80a]

4.4 - The kissing loop complex was subjected to extensive dynamics simulations to confirm the flexibility and relative stability of the construct itself as well as preservation of complete seven base pair interaction between the kissing loops.[73] Overall, the MD simulations characterized the loop-loop complex as a stable rigid motif with a unique bend which maintained the seven base pair interaction between both loops. The next step was to optimize these kissing loop motifs to construct

the core components of each side of the hexameric nanoparticle *via* the addition of RNA sequences to form helices capped with the kissing loops. The authors went on to design two different core building blocks either helices capped on either end with an RNAI loop sequence or RNAII loop sequence or helices capped with one RNAI loop sequence and one RNAII loop sequence.[73] In agreement with the 3D modeling, hexamers can be formed when the loops correspond to those of the RNAI/IIi kissing-loop complex.[73, 85]

4.5 - Although computational analysis of the proposed RNA nanorings constituted an integral component of RNA architectonics and nanoparticle design, further experimental analysis provided the means to validate and refine theoretical models for pragmatic application.[73, 86] The computationally proposed hexameric RNA nanorings were further explored and characterized in 2011 by Grabow et al.[77f] The authors reported the synthesis and characterization of various hexagonal RNA nanoparticle designs based on the modular RNAI/II kissing complexes, along with the design of a fully programmable hexameric RNA nanorings with six specific kissing loop interactions.[77f] Following the original intended proposal of using the RNA nanoparticles as the drug delivery platform, the next step was incorporation of siRNA payloads into the RNA rings. Two orthogonal strategies were used to functionalize the nanoring with Dicer Substrate (DS) RNAs with each method tested for their ability to be processed by Dicer and release siRNAs.[77f, 87] The first strategy was to encode the DS RNA in the helical backbone of RNA rings. This was made possible by extending the helical backbone from 15 bp to 26 bp (11 bp or one full helical turn) to contain the siRNA sequences while still maintaining the planarity of the kissing loop complex interactions.[77f] The second strategy was to extend the 3' end of the monomer RNA sequence with an added DS RNA strand. The same strategy is more general can be readily applied to other RNA nanoparticles.[83, 88]

These two strategies resulted in the formation of siRNA carrying RNA nanoparticles that were open to processing by Dicer while allowing precise stoichiometric control of the siRNA payload. Moreover, all functional RNA nanoparticles were shown to be produced co-

transcriptionally.[89] Furthermore, the combination of six total different siRNAs allowed for a combinatorial approach for RNAi mediated therapeutic gene silencing, which has been proven for efficient downregulation of specific gene expression and enabled versatile functionalization of the nanoparticles through swapping of functional monomers.[90] One potential drawback of the aforementioned approaches however, was the limitation for number of the potential DS RNA payloads. Although this was enough for six different DS RNAs to be attached, potential steric clashes prevented functionalization of both the 3' and 5' ends, limiting the siRNA to monomer ratio at 1:1 (six total) (Figure 5).

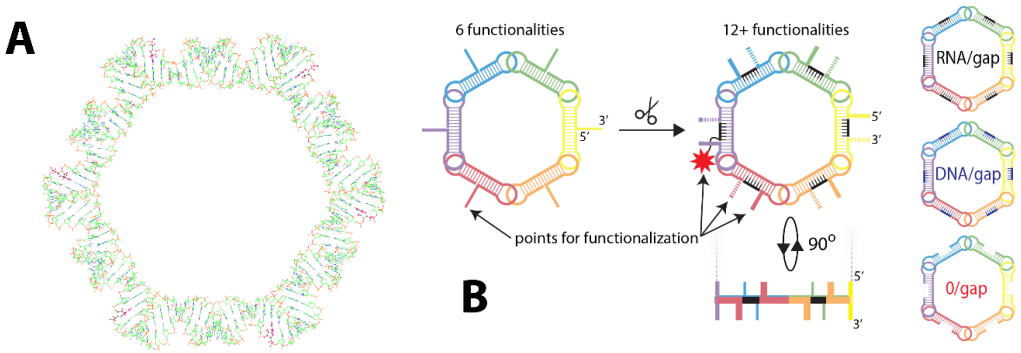

Figure 5. 5A. Basic structure of hexameric RNA nanoparticle with the spaced 3' and 5' ends of the monomers marked in red and yellow constructed with SwissPDB image software and viewed in PyMol. 5B. Visualization of the removal of six nucleotide segments and the resultant 'nicked' (shown as the black segment) RNA nanoparticle with the potential to support up to twelve+ functionalities. Given a ~33° turn per base of RNA, the removal of 6-nts from the backbone also reduces steric hinderance of potential adducts with the 5' and 3' terminal ends pointing 197° away from each other, relative to the plane of the ring.[91]

4.6 - To address the issue of being limited to six points of functionalization, we implemented a structural optimization of RNA ring scaffolds via removal of three nucleotides from both the 5' and 3' sides[91] to increase the avenues for functionalization from six to a total of 18, by not only opening up the 5' and 3' ends of the monomer, but also enabling functionalization of the six-nt single stranded "gapped" region with a nucleic acid complement strand. The introduction of the six-nt single stranded RNA (ssRNA) increased the overall flexibility of the hexameric RNA nanorings.[91] Similar to the approach taken by Yingling and Shapiro in their initial development of

the ring, different computer modeling methods played a role in the optimization of the modified nanostructures and their respective derivatives.[73, 86, 91] However, despite the promising computer-assisted predictions, experimental corroboration is often challenging and requires non-traditional characterization techniques compared to traditional characterization techniques shown in Figure 6. One such nontraditional method is the use of AFM image analysis to determine variability of the hexameric nanoring system.

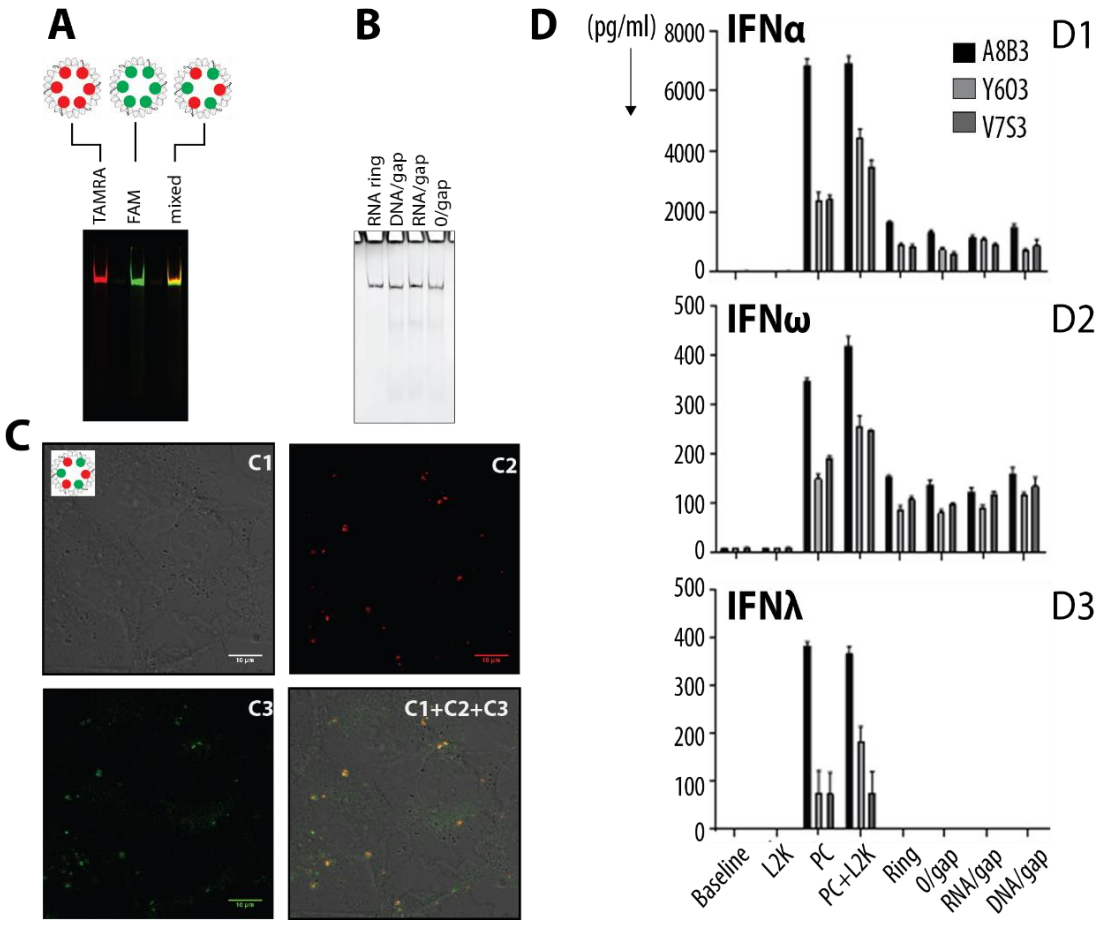

Figure 6. 6A. Native PAGE analysis of left to right: Control RNA rings, 6nt DNA nick rings (DNA/gap), 6nt RNA nick rings (RNA/gap) and 6nt nick (no nick). 6B. Functionalization of the rings with fluorophore labeled 6nt backbone sequences that (left to right) green, red, and alternate segment functionalization (green and red) to form yellow. Alternate segment functionalization is used to corroborate the structural integrity of rings during the intracellular co-localization in human breast cancer cells (C1-C3, C1+C2+C3(Images overlaid)) showing different color filters applied (Cell Line: MDA-MB-231). Figure D1-D3 display immunological studies which were conducted in vitro using PBMC derived from three healthy donors (A8B3, Y6O3 and V7S3). ODN2216, a known potent inducer of type I Interferons (IFN)s was used as the assay positive control (PC). Untreated cells were used to establish a baseline. Lipofectamine (L2K) of the same concentration was used to deliver the nanorings was used as a negative control. Both ODN2216 and L2K were also tested together to rule out any negative effects on cell viability and IFN induction when both the delivery vehicle and the IFN inducing sample are added to cells together. Nanoparticles with various modifications (Ring, 0/gap, RNA/gap and DNA/gap) were delivered using lipofectamine. Type I IFN (IFNα (Figure D1) and IFNω (Figure D2)) and type III IFN (IFNλ (Figure D3)) were analyzed in the supernatants 24 hours after addition of test samples and controls to PBMC cultures. Each bar represents a mean and standard deviation (N=3).[91]

The sensitivity of our designed AFM-based quantification approach shown in in Figure 7 was then compared to conventional physicochemical characterization of RNA nanoparticles (native-PAGE and DLS) as well as immunorecognition assays (Figure 6) which did not seem to have much distinguishable difference between each of the ring types. To explore the physical differences at a more sensitive physical level, we used AFM to evaluate the variations in relative flexibilities of each modified RNA nanostructure via deformation analysis with a high throughput of analyzed nanostructures (Figures 7 and 8).

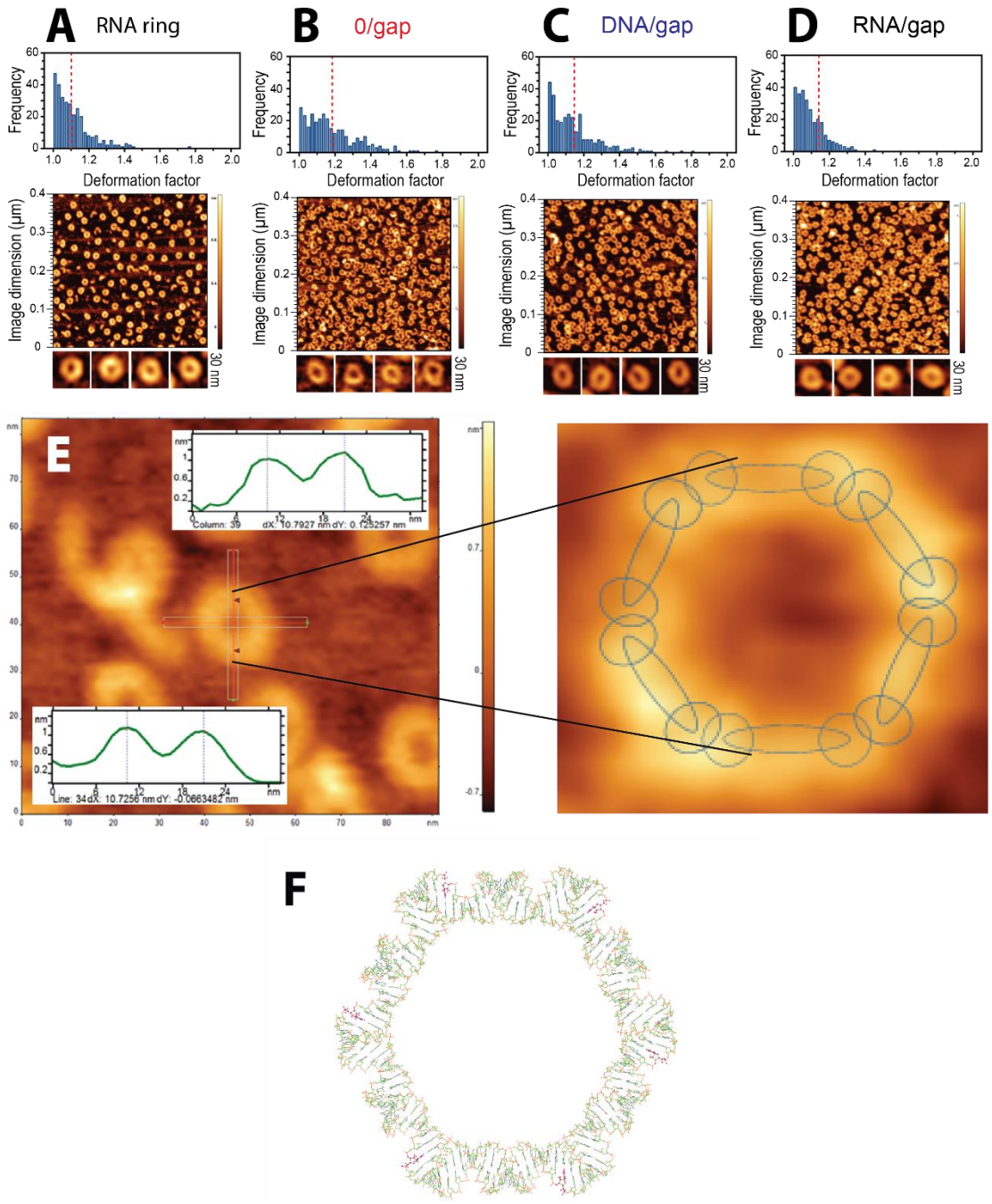

Figure 7. Ring deformation distribution histograms and AFM Images. Deformation factor is calculated as a ratio of distances between RNA ring segments for perpendicularly placed axes that cross through the center of the ring. Shown on the top panel are the Deformation Factor (DF) histograms, with the median marked with a red dashed line, for 4 types of nanostructures (7A) RNA rings (DF = ~1.1), (7B) 0/gap rings (DF = ~1.18), (7C) DNA/gap rings (DF = ~1.14), and (7D) RNA/gap rings (DF = ~1.11). Shown below the histograms are the AFM images used to calculate deformity distribution. Shown in 7E is an overlay of the hexameric dumbbell ring structure on a single AFM imaged ring. 7E demonstrates the AFM tip displacement measurements taken in order to measure the aspect ratio of the imaged rings with the peaks indicative of ring segments of the original ring (7F). This was also done with computational algorithmic deformation analysis displayed in figure 8E and 8F.[91]

As shown in Figure 7, manual AFM image analysis confirms computational predictions that the DNA/gap and RNA/gap rings have a tighter deformation factor distribution, indicating their limited flexibility when compared to the 0/gap rings. This could allow for dynamic flexibility changes of a hydrogel where the flexibility would decrease when in the presence of the complement strands and vice versa.

For statistical analysis, our newly developed AFM-based approach centered on the use of an automated image analysis algorithm for which we employed previously explored pattern-matching and segmentation techniques, utilized in biomedical image analysis (Figure 8).[92] This algorithm consisted of three steps: 1) detection of individual objects 2) differentiation of the detected objects based on set program parameters and 3) computationally derived statistical analysis of each nanoscale object.[91]

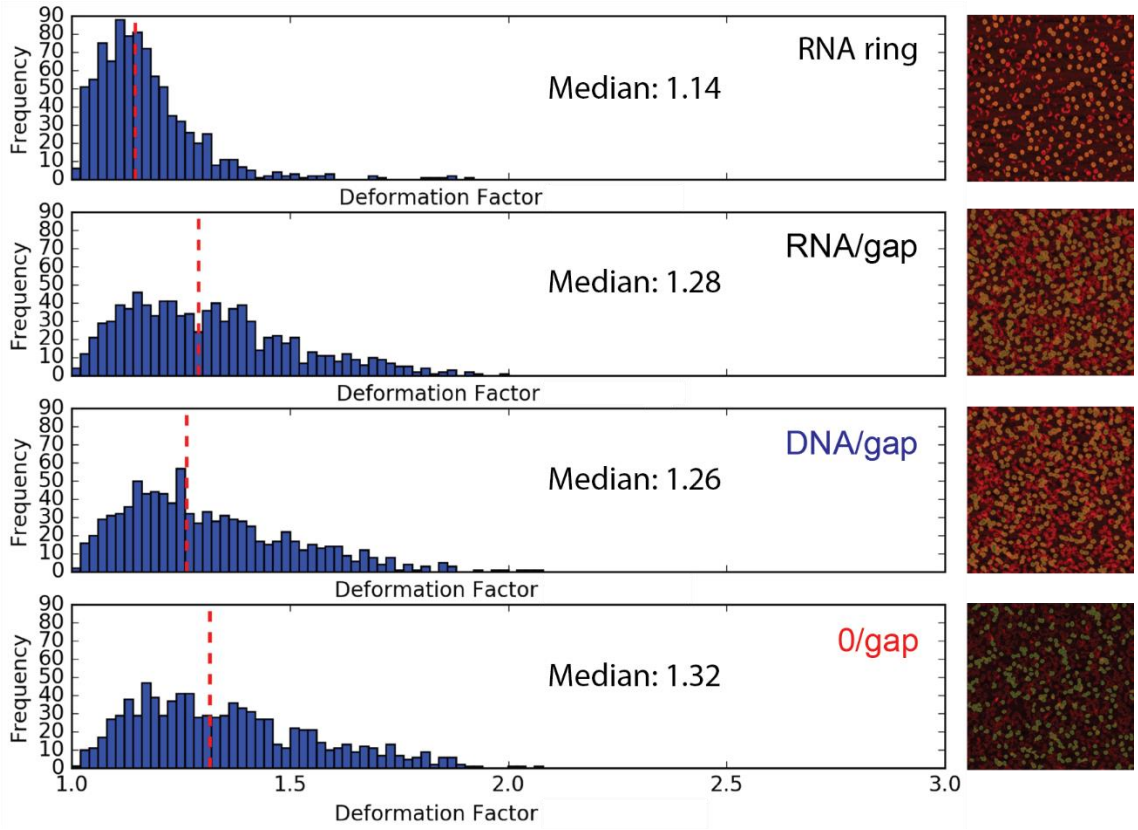

Figure 8. Computational algorithmic deformation analysis was used to determine distribution of ring deformity. Shown in figure 8 are the Deformation Factor (DF) histograms with the median marked with a red dashed line for 4 types of nanostructures, From top to bottom, figure RNA Ring (~1.14), RNA/gap (~1.28), DNA/gap (~1.26), 0/gap rings (~1.32). Shown to the right of the histograms are the AFM images with colored nanostructures selected by the algorithm used in the deformation analysis. A higher median deformation factor is indicative of more 'deformed' or more flexible rings. The control RNA rings demonstrate the least flexibility with a median deformation of 1.14. The RNA/gap and DNA/gap rings each have an increased deformation factor of 1.28 and 1.26 respectively, a greater flexibility than that of the RNA control ring but less than that of the 0/gap ring at 1.32. This indicates that different nick strands impact the flexibility of the rings themselves overall.

Above all, the results of this study improved the rational design and characterization of highly flexible RNA nanoparticles by combining traditional characterization with more sensitive and reliable approaches capable of detecting minute structural variations in nanoparticles that conventional characterization may not detect. This gap-complementary strand approach can also be incorporated into other structures as a modular avenue for functionalization with little secondary structural impact. The flexibility of the nanoring as well as their amenability to functionalization makes them a suitable candidate as a crosslinking component in an actin hydrogel. Overall, from

the results shown in Figures 4-6, we have demonstrated the functionalization of the nanoring monomers with fluorophore labeled nick strands as well as the impact of different nicked complements and their respective impact on the flexibility of the ring. These hexameric RNA nanorings would serve as dynamic crosslinking components of the proposed actin-biomolecule hydrogel (Figure 9).

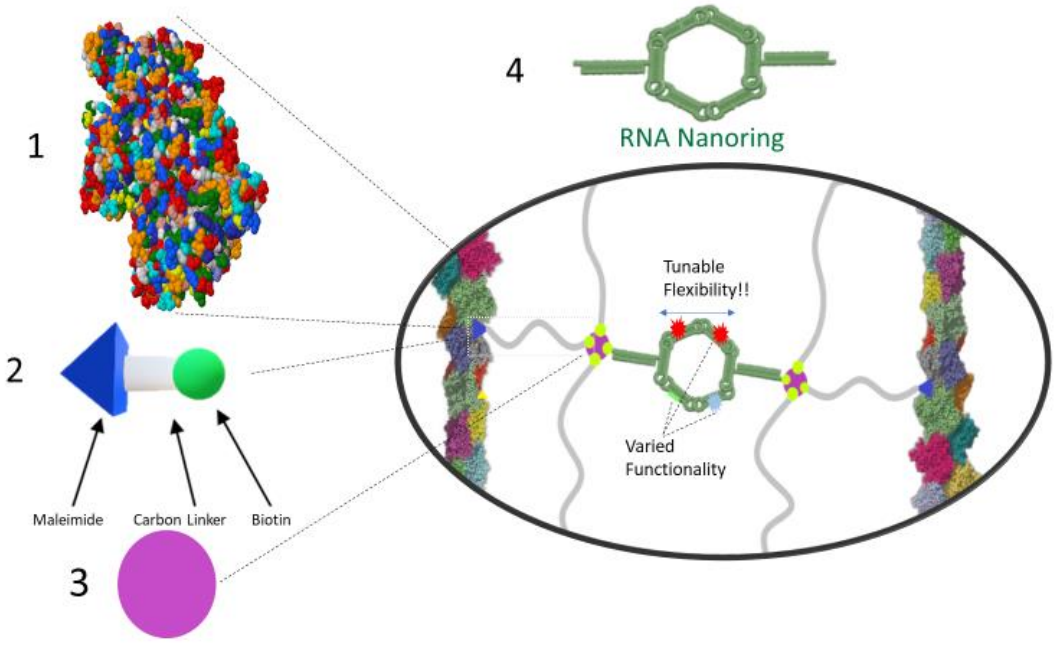

Figure 9. Application of RNA nanoring as crosslinker for a hydrogel with different functionalities embedded in the backbone of the nanoring via the nicked structure. The 1) Actin backbone would be made up of polymerized F-actin monomers, with 4) Cysteine-374 chemical handle on actin 3) Biotin functionalized linker with a malemide would allow for the incorporation of 5) Nanorings via Biotinylated functionalities added to the nicked nanoparticles which as demonstrated in figure 5, would help modulate the functional and dynamic behavior of the gel.

One of the main goals of our hydrogel exploration was to incorporate responsiveness and functionality via programmable nucleic acid crosslinks. As changes in lengths and flexibilities of individual entities (*e.g.*, RNA nanorings with ssRNA gaps in their structure) can be precisely controlled, their use as crosslinking entity in hydrogel structure is expected to greatly influence the overall physicochemical and mechanical characteristics of the hydrogel. To explore this, we aimed to utilize a nucleic acid – actin bioconjugation technique to functionalize the actin fibers with

programmable hexameric RNA nanoparticles. This would be done through conjugation of a maleimide functionalized RNA strand onto an exposed cysteine residue on actin (Cystiene-374). A dynamic nucleic acid hydrogel was previously explored by Cangialosi et al.[93] where the authors introduced a programmable swelling based on DNA hairpin crosslinker interactions. We hypothesized that incorporation of our hexameric RNA nanoparticle would not only introduce multiple avenues for functionalization at a single crosslinking point but also enable tunable flexibility via the introduction of six-nt gap complement (Figure 9).

CHAPTER 5: BIOCONJUGATION

5.1 - As emphasized in Whitesides work, an important step in the exploration of creating a biomolecule hydrogel is the identification of a suitable bio-conjugation strategy for the synthesis of protein based nanomaterials.[22, 94] To synthesize a hybrid protein-nucleic acid nanomaterial, it is of utmost importance to identify an effective method to unite various molecules together in an organized, quantifiable manner.[21, 28, 35] Bioconjugation strategies generally are of two types – covalent and non-covalent binding – each with their own scope of application similar to the difference between the covalent synthesis of hydrogels developed by Peppas vs the 'self-assembling' materials detailed by Whitesides.[13b, 22]

5.2 - Covalent linking, involves linking of different surface exposed chemical moieties with specific groups on other molecules to create covalent bonds.[94] In most scenarios, covalent bioconjugation tools attempt to bind to a target moiety on a substrate such as: a surface exposed native amino acid residue, terminal amine/carbonyl group, reactive moieties or an artificially engineered reactive groups on a biomolecule.[94] By using the amino acid residues native to a protein, bioconjugation may be achieved without previously altering the protein itself, reducing the risk of altered functionality as an unforeseen side effect of additional reaction steps.[95] In the experiment presented, we focus on using a cysteine residue (C374) displayed in Figure 10, offering the potential for bioconjugation via thiol chemistry while simultaneously being chemo-selective due to the rare presence of surface exposed cysteines on actin.[96] The selection of a specific amino acid residue target was based on the identification of a suitable chemical handle for bioconjugation chemistry with actin as the protein of focus.

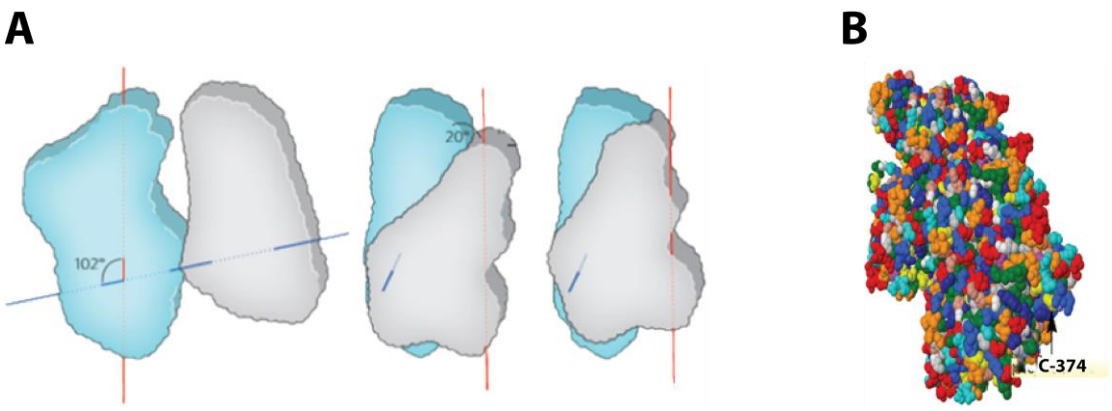

Figure 10. 10A. Diagram of G to F-actin conformational change. 10B. F-actin atomic structure with C374 identified[44] This demonstrates conformation dependent exposure of the Cystiene-374 which would act as a chemical handle for crosslinking via thiol-maleimide chemistry.

5.3 - Actin itself has one surface exposed cysteine at residue position at 374, though this is only exposed in the fibrous (F) conformation of actin.[31 38b, 45] This is ideal for bioconjugation with a target residue, as it offers high structural specificity; with actin possessing a single cysteine exposed only in the fibrous conformation, this strategy allows for the use of bio-orthogonal thiol binding chemical partners without potential for alternate binding sites. Furthermore, the single cysteine is exposed only in the fibrous conformation, which enables potential crosslinking-suitable bioconjugation techniques to be employed. Binding only in F-conformation allow for crosslinker-binding with other actin fibers rather than globular actin molecules, which is much more suitable for a crosslinked hydrogel structure built with interconnected fibers without the possibility of unwanted crosslinking to unbound terminal ends.

5.4 - Once the target group was identified, it was important to find a suitable chemical linking strategy to perform the bioconjugation since cysteine has a few potential chemical binding partners, each of which reacts with the thiol functional group.[97] Maleimides were selected as functional binding partners (Figure 11) due to their well-established synthetic foundation, high binding selectivity towards thiols, and biorthogonal nature.[98]

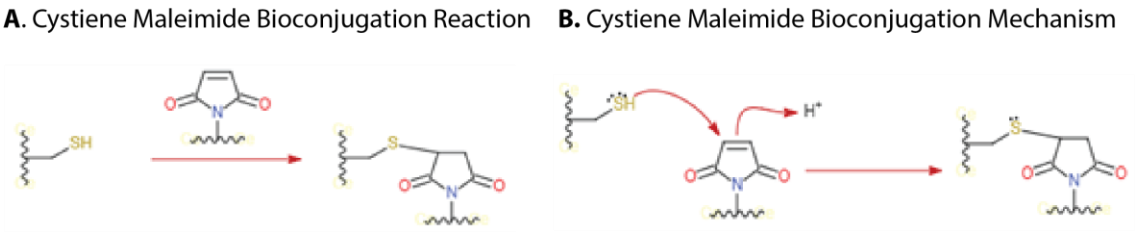

Figure 11. 11.A Cysteine and Maleimide Reaction. 11.B Electronic mechanism of Thiol-Maleimide Michael Addition which would be used to conjugate the Cys-374 shown in Figure 11B.

Having selected this binding partner, one strategy was used to synthesize maleimide-functionalized oligonucleotide strands: a commercially-available labeled DNA from Genelink shown in Figure 12A, along with potential other functionalization strategies for different bioconjugation targets.[99] This covalent linker would be used to conjugate complementary oligonucleotide strands to actin to act as nucleic acid crosslinking components via base pairing.

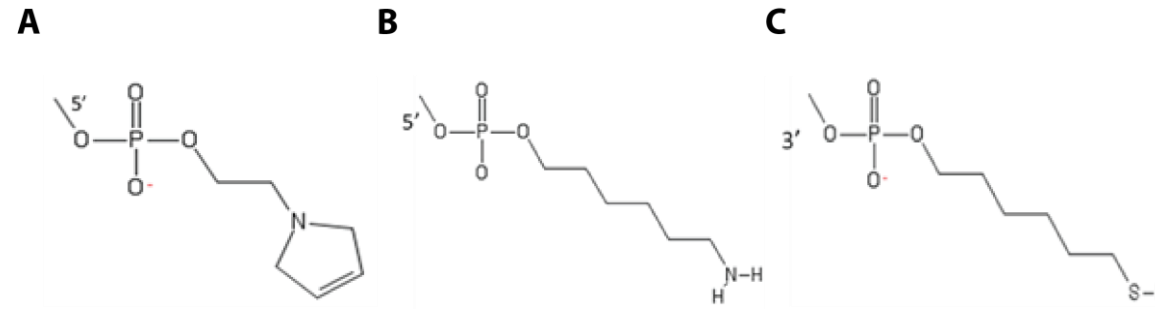

Figure 12. Reagents used in Nucleic Acid Bioconjugation: 12.A. Commercial 5' Maleimide-Oligo (Genelink). 12.B. 5' Amine-Oligo, 12.C 3' Thiol Modified Oligo

5.5 - The initial foray into synthesizing an actin-based hydrogel structure began with the employment of the commercially available 5' maleimide-functionalized oligonucleotide strand. The goal for this experiment was to utilize the surface exposed 374 position cysteine as a chemical handle to attach maleimide functionalized complementary oligonucleotide strands. These complementary strands, attached to different actin monomers, would then undergo spontaneous base pair hydrogen-bonding and serve as crosslinks to the actin, schematically shown in Figure 13. This is the proof of concept for further exploration of nucleic acid crosslinks which could be tuned

for increased functionality as mentioned previously with incorporation of RNA nanoparticles and aptamers.

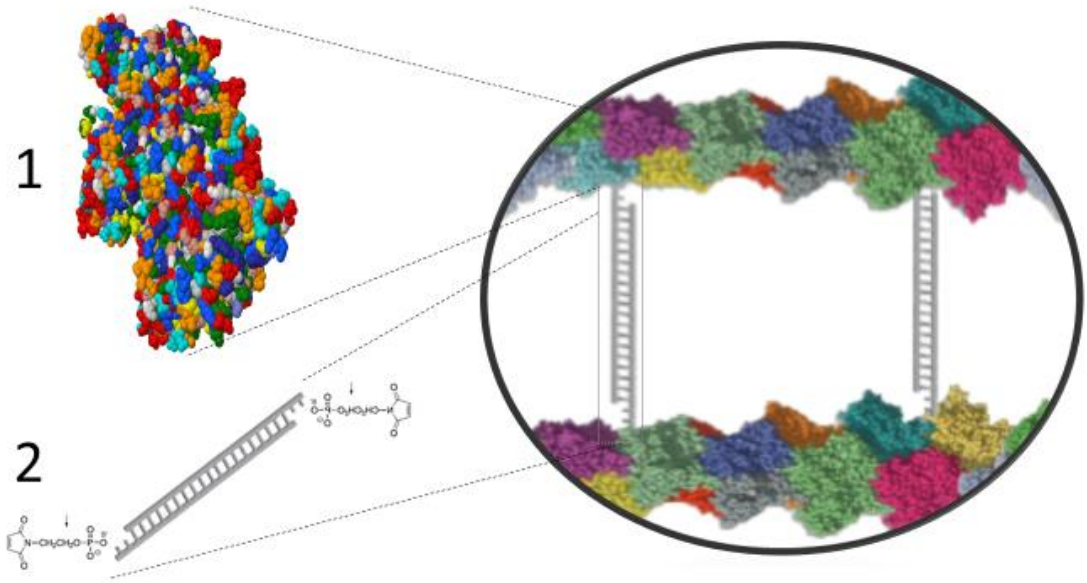

Figure 13. Schematic of DNA-actin Hydrogel with commercially available 5' Mal-Oligonucleotide Duplex. 1) Actin monomer 2) 5' Maleimide functionalized Oligonucleotide Duplex. Shown here is the DNA duplex acting as a crosslink between 2 actin fibers via conjugation to the Cys-374 on each fiber.

5.6 - Actin Hydrogel Characterization - The following were characterized on a Native PAGE (Polyacrylamide Gel Electrophoresis) in a 37.5:1 Acrylamide: Bisacrylamide with 2 mM Mg2+ ion concentration in gel. The gels were stained with Ethidium bromide before being imaged under UV light. The duplex actin -DNA- actin construct was sent for AFM and included below in Figure 14.

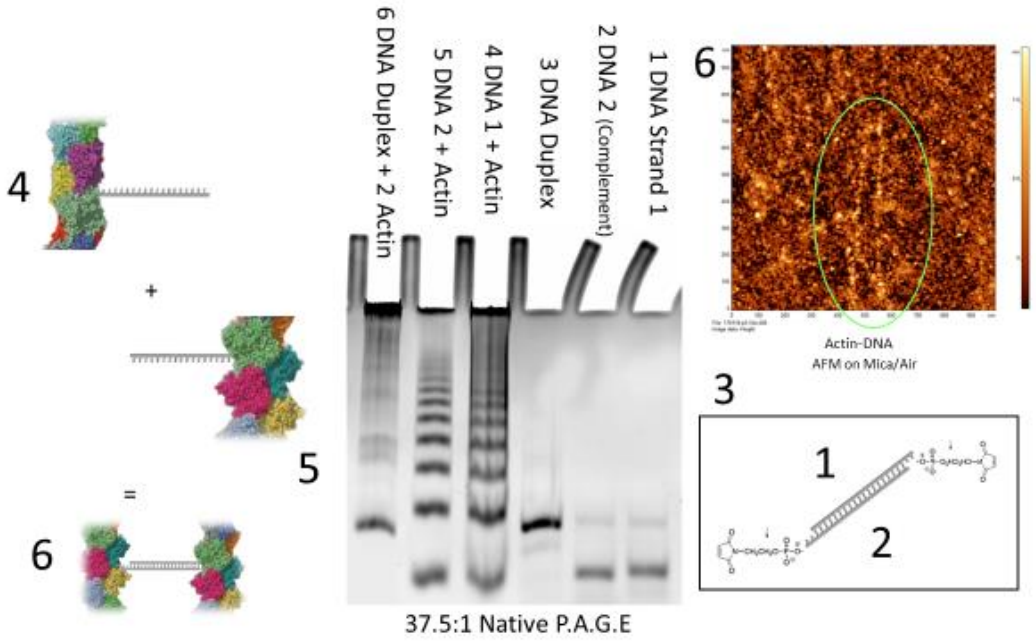

Figure 14. Overall scheme of the results of the bioconjugation attempts using the 5' commercially available linker. Shown above are the lane labels with each component labeled accordingly. Lane 1 and 2 show the DNA strand and complement strand, which together form the DNA duplex shown in Lane 3. These DNA strands were each conjugated to C374 on an actin monomer and run through Native PAGE. The actin conjugated with the DNA sense strand (Lane 4) and the antisense strand (Lane 5) are combined to form the actin-DNA-actin Duplex (Lane 6). This duplex structure was sent for AFM and is shown in the AFM image as well as represented by Lane 6.

5.7 - This experiment was the first steps in attempting to covalently link an oligonucleotide strand to actin in order to utilize its natural base pairing as a crosslinking strategy. The maleimide functionalized DNA strands, complements of each other, only worked partially well in terms of creating a linked actin structure, however the lack of definitive results caused us to attempt other strategies that would prove to be more successful. The experimental attempts to purify and isolate the actin-DNA conjugates as well as confirm our polymerization and work up strategies are all outlined in the Appendix along with further experimental detail and corresponding data.

CHAPTER 6 - VISUALIZATION OF HYDROGEL FORMATION VIA "BROCCOLI" RNA APTAMER

6.1 - Visualization techniques are equally important in biotechnology, as they allow for the tracking of various processes and products in different biological systems. Most widely known techniques in molecular biology employ the use of Green Fluorescent Protein (GFP). Originally isolated from the jellyfish *Aqueorea Victoria*, it has changed way visualization of proteins and nucleic acids is accomplished.[100] GFP is an useful tool for biological visualization because of its ability to form an internal chromophore without requiring any biological accessory, enabling it to be a self-contained fluorescent reporter.[101] Roger Y. Tsien, Osamu Shimomura, and Martin Chalfie, were awarded the 2008 Nobel Prize in Chemistry for its discovery.[100, 102] The GFP gene can be linked to a regulatory sequence of another gene of interest and then used as an indication of whether a certain gene has been taken up by or expressed in the target population of both prokaryotes and eukaryotes.[100b, 103] Visualizing GFP is simple and noninvasive, requiring only illumination with blue light and GFP alone does not interfere with biological processes and is able to diffuse readily throughout cells.[100a, 100b] The GFP sequence was modified and optimized to be more practical for use as a visualization tool. The first major improvement to the GFP system was a single point mutation where serine at position 65 was changed to a threonine.[104] This mutation significantly improved the spectral characteristics of GFP and resulted in increased fluorescence and photostability and shifted the major excitation peak to 488 nm, with emission kept at 509 nm.[104] This modification increased the practicality of use by other researchers. Many other modifications were made with the goal of increasing its applicability. Another very important modification was the development of superfoldGFP by Cabantous et al, which enabled GFP to fold even if it was linked to poorly folding proteins.[105] This in turn enabled better utilization as a quantification tool. In order to even further increase its applicability, they also developed the split GFP system.[106] This system works by incorporating 2 halves of the GFP protein into a binary reporter system, where each half, in proximity of its counterpart, can form the full GFP, but neither fluoresces on its own.

Each of these halves is fused to a protein of interest. This enables the fluorescent signal corroboration of colocalized proteins; a fluorescent signal indicates the close spatial proximity of each of the target proteins due to the two halves of GFP coming together to create a fluorescent signal..[106]

6.2 - For visualizing intracellular RNAs, the genetically fused MS2-GFP proteins have been utilized to tag and image endogenous RNAs in cells via MS2 binding to sequence specific RNA hairpins.[107] However, this approach requires tagging RNAs with multiple copies of fused MS2-GFP systems in order to improve the signal to noise ratio, which has the potential to affect the mobility of labeled RNAs and alter their function. Using several proteins with fluorescently labels as FRET (Förster resonance energy transfer) pairs is another possible way for nucleic acid nanoparticle (NANP) visualization but may require the presence of bulky tags and may be limited in their functional applications and utility.[108] NANPs can be directly visualized in living cells using complementary strands labeled with pairs of dyes that can undergo FRET.[109] This fluorescent signal change that rely upon dynamic re-hybridization of these strands becoming part of the target NANP can be used to visually confirm the dynamic behavior of these nanoparticles.[82-83, 109-110] Likewise, the integrity of the target NANPs in cells can be confirmed through co-localization of multiple different fluorophore labeled strands with potentially the same consequent fluorescent signal if designed correctly.[91, 111] However, for all mentioned techniques, the fluorescent dyes must be covalently (chemically labeled complement strands) or non-covalently (MS2-GFP system) linked to either the 5′- or 3′-end of nucleic acids, limiting the application of these techniques. Therefore, the advancement of NANP's in the current research context must be augmented by further developments in robust, biocompatible, visualization techniques and technologies.

6.3 - RNA Aptamers are specific nucleic acid sequences that are selected to bind with a high affinity to target molecule of interest.[3e, 50, 82] Common aptamer targets include proteins, peptides, small molecules and many other compounds. [3e] The development of RNA aptamers has been a major improvement over other imaging techniques. These aptamers, which activate

fluorophores upon binding, offer improved signal-to-noise ratios, increased modularity for simple application, and peptide free imaging in cells.[112] These are developed through in vitro selection or SELEX (systematic evolution of ligands by exponential enrichment). SELEX is the process in which randomly generated sequences are experimentally selected for their affinity against a target molecule.[113] Through repeated sets of affinity chromatography, the sequences which do not have binding capability are removed and the remaining sequences are amplified and analyzed. These sequences are put through a more stringent selection procedure to find the tightest binding partner for the target molecule. SELEX was used to select a unique RNA sequence which binds and activates a normally non-fluorescent dye (Malachite Green), which was developed into an optimized aptamer by Afonin et al. under the concept of token-RNAs.[77d, 114] This was developed in order to increase the fluorescent emission of the Malachite Green dye to augment its use as a visualization tool for nucleic acids. The MG aptamer was also investigated and developed into a split aptamer system, analogous to the split GFP system by Kopashikov et al.[114-115]

Because these aptamers are composed of nucleic acids, they can act as modular functional units which can be easily embedded into a NANP's structure via simple extension of individual NANP component strands.[109] This offers a myriad of demonstrated benefits in terms of characterization and quantification of NANPs including tracking co-transcriptional assembly, assembly verification, and monitoring the dynamic behavior of interdependent RNA-DNA hybrids.[90c, 110, 116] However, drawbacks of the MG system, including its high cytotoxicity of MG and its non-specific binding to other molecules in the cell, warranted the search for new biocompatible RNA aptamers, especially those which could be used at a higher concentrations without adverse effects. In their exploration of a potential nontoxic RNA aptamer to act as a mimic of GFP, Jaffrey et al. designed and developed the Spinach RNA aptamer. Using SELEX, the Spinach aptamer was selected to bind a GFP fluorophore analog, the dye (Z)-4-(3,5-difluoro-4-hydroxybenzylidene)-1,2-dimethyl-1H-imidazol-5(4H)-one (DFHBI), and to exhibit green fluorescence only when bound to the RNA aptamer.[117]

Spinach was further optimized into Spinach2 for increased fluorescent signal and stability, yet still required a tRNA scaffold to promote folding and stability which makes it susceptible to endonucleases and limited cellular activity.[118] To increase its binding with DFHBI-1T and consequent fluorescent signal, the Jaffrey group fine-tuned Spinach2 into an even shorter aptamer called Broccoli.[119] Broccoli demonstrates a significant improvement because of its selective evolution. Its advantages include relatively higher thermostability, expression level, and a shorter sequence as well as improved efficacy in in vivo studies given its lower magnesium dependence, which reduced potential magnesium interference with cellular functions.[117, 119b, 120] The modified F30 scaffold on Broccoli enhances its fluorescence while also not being as bulky as the tRNA scaffold required for Spinach2. Similarly, like applications of the split GFP system, split RNA aptamers have been demonstrated in many areas, including biosensing, tracking the assemblies of RNA nanoparticles and the conditional activation of split functionalities.[80b, 86a, 109-110] To assess the actions of dynamic NANPs, RNA aptamers were also split such that fluorescence is restored only upon the subsequent halves of the aptamer being brought into close proximity to re-associate and bind to a dye. For example, Halman et al. split the F30 Broccoli aptamer into two separate strands which are inactive when separate but bind the small dye DFHBI-1T upon reassociation, shown conceptually in Figure 15.

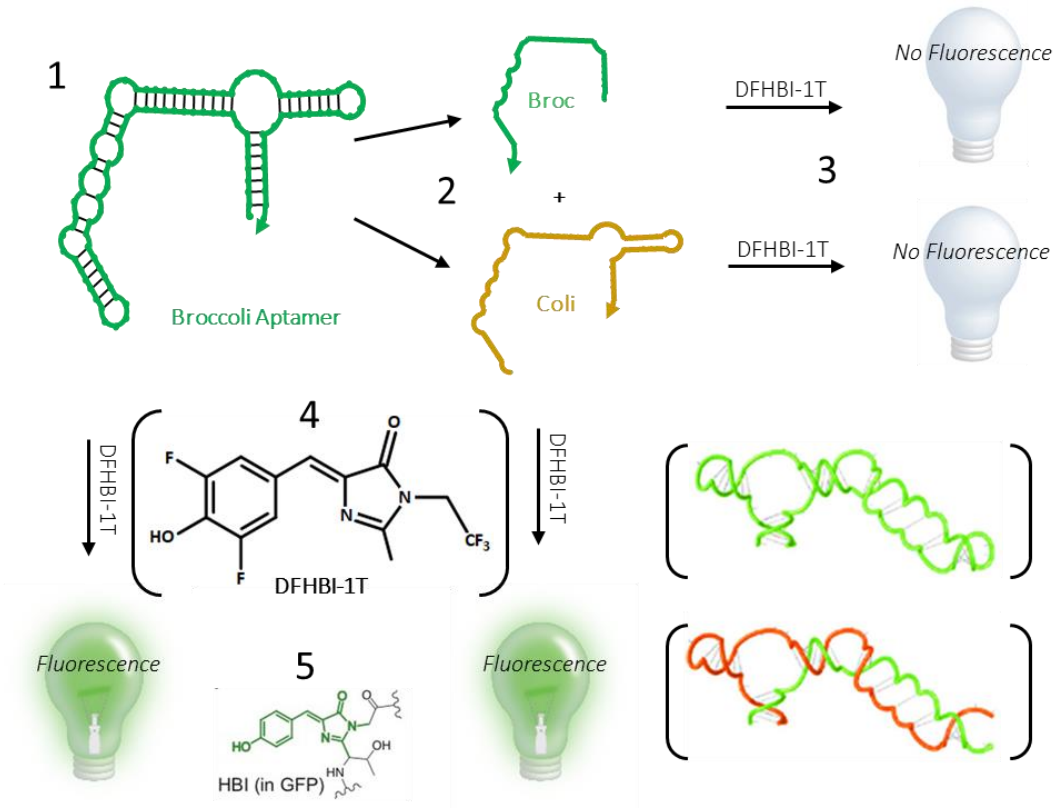

Figure 15. Broccoli aptamer structure and schematic illustrating conditional fluorescence upon reassembly of Broc+Coli in the presence of DFHBI-1T fluorophore. From 1) The Broccoli aptamer is made up of 2 parts, shown in 2) Broc (in green) and Coli (in orange) with 3) conditional fluorescence based on aptamer formation and molecular affinity for 4) DFHBI-1T. DFHBI-1T is a mimic of the naturally occurring fluorophore 5) HBI in GFP. This figure indicates conditionally activated fluorescence of the Broccoli aptamer when assembled (Broc+Coli) as well as the necessary presence of the fluorophore DFHBI-1T [121]

Halman et al. then used the split Broccoli aptamer to demonstrate its use as an optimized aptameric tool for the purpose of visualizing the dynamic interactions between NANPs.[109] Further exploration of the G-quadruplex structure of the Spinach aptamer, involved in binding DFHBI, resulted in the sequence of Spinach being truncated into Baby Spinach while exhibiting comparable fluorescence.[119b] Chandler et al. then set out to optimize the split F30-Broccoli aptamer experimentally in order to produce several conditionally activated splits, called florets (REF), that would enable elucidation the underlying properties of DFHBI-1T binding and fluorescence in regards to the Broccoli structure, without the complexities of solving for multiple DFHBI-1T-Broccoli cocrystal complexes.[111, 119a, 120c, 122]

As shown in Figure 16, DFHBI-1T only fluoresces when in the presence of the fully assembled aptamer, demonstrating conditional fluorescence. [121]

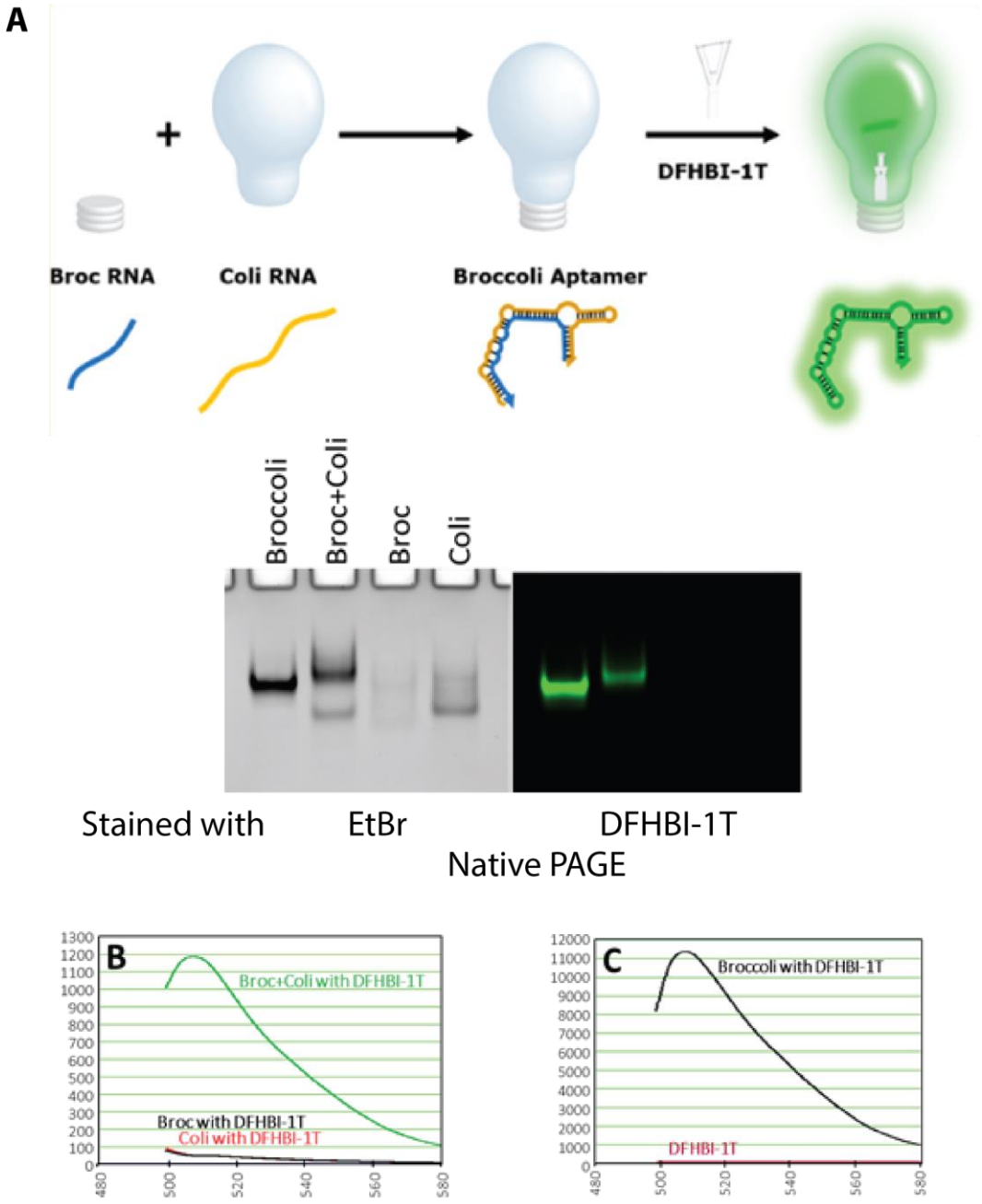

Figure 16. Visualization of Broccoli fluorescence in Native PAGE via Ethidium Bromide for Nucleic acids and UV irradiation for conditional fluorescence. Shown here is the demonstration of assembly dependent formation. The aptamer fully assembled, is shown stained with Ethidium Bromide to visualize the DNA and irradiated under UV light for bound DFHBI-1T-Aptamer fluorescence. Lanes 3 and 4, each only containing 1 of the components of Broccoli, do not express DFHBI-1T fluorescence due to the lack of aptamer formation. A conceptual schematic is shown to the right, illustrating the behavior of the split aptamer with fluorescent measurements of both nonfluorescent components, as well as the assembled aptamer, each when in the presence of DFHBI-1T [121]

This approach to synthetic aptamers demonstrates the general strategy for conditional re-activation of disconnected functional ssRNAs with complex secondary structure for the purpose of creating dynamic RNA nanostructures. This was later refined and modified to be a pedagogical tool, as demonstrated by Sajja and Chandler et al. in the design and conception of a novel chemistry lab at UNC Charlotte that utilizes the reassociation-based fluorescent activation of the aptamer itself.[121] Usage in a laboratory setting serves as a testament to the consistency and robust nature of the split aptamer system. Employing the same bioconjugation strategies utilized in this experiment, the use of the aptamer as a crosslinker would allow for fluorescent tracking of crosslinking by way of a fluorescent signal and visual confirmation (Figure 17). Further, utilizing the "Broc+Coli" aptamer as a crosslinker would have even greater value, as the aptamer would only fluoresce upon reassembly.

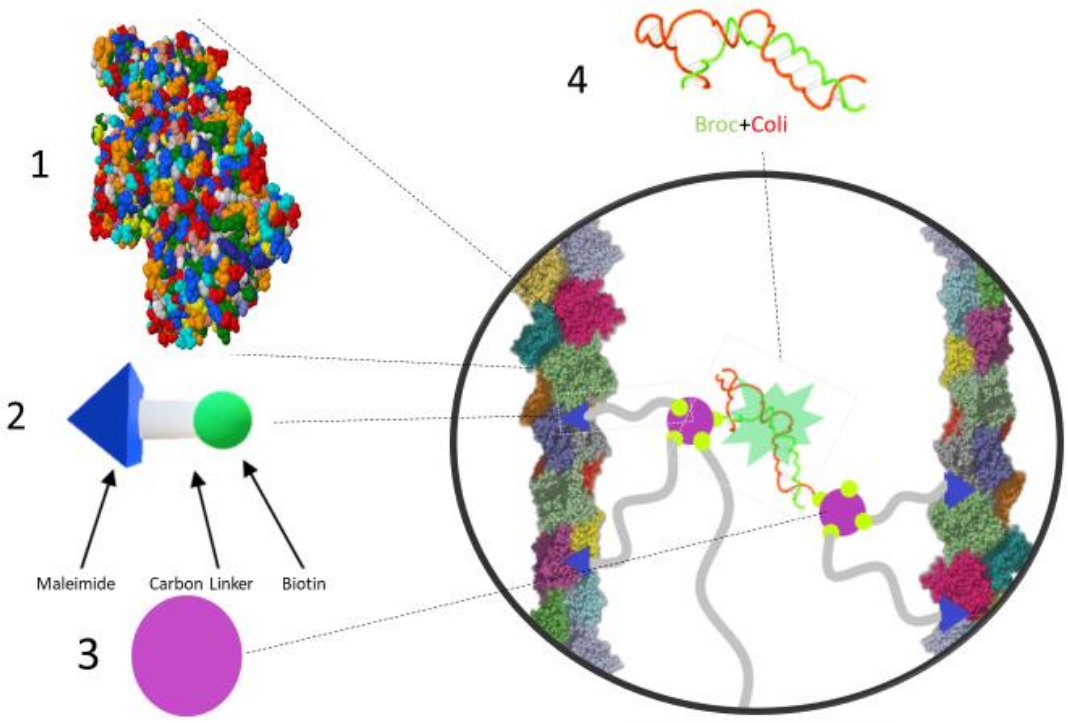

Figure 17. Here is a conceptual schematic of actin fibers crosslinked with the split broccoli aptamer. Shown above is 1) actin fiber stabilized with a 3)biotin functionalized maleimide linker Streptavidin hub via a 2) Maleimide-Biotin linker. The 5) Split Broccoli aptamer, when acting as an active crosslink in the presence of DFHBI-1T, would fluoresce due to the Broccoli aptamer acting as a conditionally fluorescent crosslink which could be fluorescently quantified as demonstrated in Figure 16. A fluorescence reading would indicate crosslinking of the streptavidin hubs via the Broccoli aptamer.

CHAPTER 7 – CONCLUSION

Through our work, we have taken the nascent steps in the synthesis of a functional actin – nucleic acids hybrid hydrogels. This was done through identification of various hydrogel components, actin, biotin/streptavidin, and RNA along with the identification of the cystiene-maleimide conjugation strategy to connect all the respective parts. In tandem with the actin hydrogel synthesis attempts, the dynamic and responsive biomolecular components of the gel were synthesized and explored to better characterize their potential application. We determined the dynamic behavior change of RNA nanorings based on backbone modification as well as the assembly dependent fluorescence of the "Broc+Coli" RNA split aptamer. This inquiry achieved two of the three driving goals, as we successfully synthesized and characterized a dynamic RNA crosslinker in the form of the nicked nanorings and characterized a responsive RNA aptamer to potentially act as a crosslinking visualization tool. As we did not identify a successful bioconjugation technique, further exploration of this research should focus on the study and application of the components of the gel to characterize their potential for biomedical use as well as home in on the synthesis of an actin hydrogel prototype.

Future experiments regarding the work presented in this thesis can be organized as follows. Primarily, a physical sample of the actin-streptavidin gel should be synthesized and characterized. This is to confirm the non-covalent crosslinking technique used (streptavidin crosslinking via other biotinylated linkers) and to establish a foundation for biomolecule component incorporation into the gel. After establishing the actin backbone, the next area of focus would be the developed RNA components (hexameric RNA nanoring and the broccoli aptamer). Incorporation of the RNA components would follow the same overall strategy; functionalization of the different RNA constructs with a Biotin functional group to facilitate noncovalent binding to the central streptavidin hubs of the backbone actin structure. Incorporation of the hexameric RNA nanoring would have a few different approaches in itself; biotinylation of the ring monomers themselves, or the addition

of a biotinylated nick strand to pair with the 6nt gap in the ring backbone. Given our ability to deliberately functionalize each monomer of the hexameric ring, a nanoparticle with opposite monomers containing Biotin (monomers A and D for example) would allow for determination of the ring's varied flexibility and the resultant effect on the gel structure overall given different nicked strands. Incorporation of the Broccoli aptamer would involve biotinylation of opposite terminal ends of each of the "Broc" and "Coli" binary strands, allowing for potential crosslinking between the streptavidin hubs. The fluorescence of the Broccoli aptamer would be determined with the added biotin functional group, then with 2 flanking Streptavidin molecules, and then when incorporated into the gel itself. Similarly, assembly of the Broccoli aptamer would be tested when each Biotinylated component, "Broc" and "Coli" is attached to a different streptavidin to establish potential for assembly a crosslinking component. Each stage of aptamer testing would set the experimental basis for confirming gel crosslinking via conditionally activated fluorescence, as proposed. Lastly, the creation of a hydrogel prototype with tunable ratios of Broccoli, hexameric rings, and other added functionalization would be the final stage of the gel development. Given successful incorporation of both the Broccoli aptamer and the hexameric ring into the hydrogel, different ratios of each of the biomolecule components would be tested to establish the experimental bounds of the gel structure. Also, varying the composition of the proposed hydrogel in regards to its biomolecular payload would be essential to exploring the different effects of each component as a reflection of overall function and structure. The work done herein sets the introductory stages of the development of a 'smart' biomaterial with the direction of future experiments included to set the proper experimental context, for each developed component and the proposed hydrogel product.

REFERENCES

1. (a) Bonnell, D., The next decade of nanoscience and nanotechnology. ACS Publications: 2010; (b) Petka, W. A.; Harden, J. L.; McGrath, K. P.; Wirtz, D.; Tirrell, D. A., Reversible Hydrogels from Self-Assembling Artificial Proteins. *Science* **1998,** *281* (5375), 389-392.

2. Song, R.; Murphy, M.; Li, C.; Ting, K.; Soo, C.; Zheng, Z., Current development of biodegradable polymeric materials for biomedical applications. *Drug Des Devel Ther* **2018,** *12*, 3117-3145.

3. (a) Theron, J.; Walker, J. A.; Cloete, T. E., Nanotechnology and water treatment: applications and emerging opportunities. *Crit Rev Microbiol* **2008,** *34* (1), 43-69; (b) Renal clearable inorganic nanoparticles: a new frontier of bionanotechnology. *Mater. Today* **2013,** *16*, 477; (c) Yeates, T. O.; Liu, Y.; Laniado, J., The design of symmetric protein nanomaterials comes of age in theory and practice. *Current opinion in structural biology* **2016,** *39*, 134-143; (d) Glover, D. J.; Clark, D. S., Protein Calligraphy: A New Concept Begins To Take Shape. *ACS Central Science* **2016,** *2* (7), 438-444; (e) Rothlisberger, P.; Gasse, C.; Hollenstein, M., Nucleic Acid Aptamers: Emerging Applications in Medical Imaging, Nanotechnology, Neurosciences, and Drug Delivery. *Int J Mol Sci* **2017,** *18* (11).

4. (a) Biocompatability of carbon nanotubes with stem cells to treat CNS injuries. *Anat. Cell Biol.* **2013,** *46*, 85; (b) Feng, J.-J.; Song, Y.-Y.; Feng, X.-M.; Shrestha, N. K.; Wisitruangsakul, N., Biocompatible Functional Nanomaterials: Synthesis, Properties, and Applications. *Journal of Nanomaterials* **2013,** *2013*, 1; (c) Cellular uptake and intracellular degradation of poly(alkyl cyanoacrylate) nanoparticles. *J. Nanobiotechnol.* **2016,** *14*, 1.

5. (a) Hoffman, A. S., Hydrogels for biomedical applications. *Advanced Drug Delivery Reviews* **2012,** *64*, 18-23; (b) Caló, E.; Khutoryanskiy, V. V., Biomedical applications of hydrogels: A review of patents and commercial products. *European Polymer Journal* **2015,** *65*, 252-267.

6. (a) Sun, L.; Huang, Y.; Bian, Z.; Petrosino, J.; Fan, Z.; Wang, Y.; Park, K. H.; Yue, T.; Schmidt, M.; Galster, S.; Ma, J.; Zhu, H.; Zhang, M., Sundew-Inspired Adhesive Hydrogels Combined with Adipose-Derived Stem Cells for Wound Healing. *ACS Applied Materials & Interfaces* **2016,** *8* (3), 2423-2434; (b) Rivest, C.; Morrison, D.; Ni, B.; Rubin, J.; Yadav, V.; Mahdavi, A.; Karp, J.; Khademhosseini, A., Microscale hydrogels for medicine and biology: synthesis, characteristics and applications. *Journal of Mechanics of materials and structures* **2007,** *2* (6), 1103-1119; (c) Luo, Y.; Kirker, K. R.; Prestwich, G. D., Cross-linked hyaluronic acid hydrogel films: new biomaterials for drug delivery. *Journal of Controlled Release* **2000,** *69* (1), 169-184.

7. Lieleg, O.; Ribbeck, K., Biological hydrogels as selective diffusion barriers. *Trends in Cell Biology* **2011,** *21* (9), 543-551.

8. (a) Lo, C.-M.; Wang, H.-B.; Dembo, M.; Wang, Y.-l., Cell Movement Is Guided by the Rigidity of the Substrate. *Biophysical Journal* **2000,** *79* (1), 144-152; (b) Hadjipanayi, E.; Mudera, V.; Brown, R. A., Close dependence of fibroblast proliferation on collagen scaffold matrix stiffness. *Journal of tissue engineering and regenerative medicine* **2009,** *3* (2), 77-84; (c) Engler, A. J.; Sen, S.; Sweeney, H. L.; Discher, D. E., Matrix elasticity directs stem cell lineage specification. *Cell* **2006,** *126* (4), 677-89.

9. Murphy, N. P.; Lampe, K. J., Mimicking biological phenomena in hydrogel-based biomaterials to promote dynamic cellular responses. *Journal of Materials Chemistry B* **2015,** *3* (40), 7867-7880.

10. Wichterle, O.; Lim, D., Hydrophilic gels for biological use. *Nature* **1960,** *185* (4706), 117.

11. Bemellen, Der Hydrogel und das kristallinische Hydrat des Kupferoxydes. *Zeitschrift für Chemie und Industrie der Kolloide* **1896,** *1* (7), 1-24.

12. Wichterle, O.; LÍM, D., Hydrophilic Gels for Biological Use. *Nature* **1960,** *185*, 117.

13. (a) Peppas, N. A.; Merrill, E. W., Crosslinked poly(vinyl alcohol) hydrogels as swollen elastic networks. *Journal of Applied Polymer Science* **1977,** *21* (7), 1763-1770; (b) Peppas, N. A.; Merrill, E. W., Poly(vinyl alcohol) hydrogels: Reinforcement of radiation-crosslinked networks by crystallization. *Journal of Polymer Science: Polymer Chemistry Edition* **1976,** *14* (2), 441-457.

14. Langer, R.; Folkman, J., Polymers for the sustained release of proteins and other macromolecules. *Nature* **1976,** *263*, 797.

15. Peppas, N. A.; Merrill, E. W., Development of semicrystalline poly(vinyl alcohol) hydrogels for biomedical applications. *Journal of Biomedical Materials Research* **1977,** *11* (3), 423-434.

16. Vacanti, J. P.; Morse, M. A.; Saltzman, W. M.; Domb, A. J.; Perez-Atayde, A. R.; Langer, R., Selective cell transplantation using bioabsorbable artificial polymers as matrices. *Journal of pediatric surgery* **1988,** *23 1 Pt 2*, 3-9.

17. Langer, R., INVITED REVIEW POLYMERIC DELIVERY SYSTEMS FOR CONTROLLED DRUG RELEASE. *Chemical Engineering Communications* **1980,** *6* (1-3), 1-48.

18. Mathur, A. M.; Moorjani, S. K.; Scranton, A. B., Methods for Synthesis of Hydrogel Networks: A Review. *Journal of Macromolecular Science, Part C* **1996,** *36* (2), 405-430.

19. Brannon-Peppas, L.; Peppas, N. A., Solute and penetrant diffusion in swellable polymers. IX. The mechanisms of drug release from ph-sensitive swelling-controlled systems. *Journal of Controlled Release* **1989,** *8* (3), 267-274.

20. Peppas, N. A.; Khare, A. R., Preparation, structure and diffusional behavior of hydrogels in controlled release. *Advanced Drug Delivery Reviews* **1993,** *11* (1), 1-35.

21. Peppas, N. A.; Bures, P.; Leobandung, W.; Ichikawa, H., Hydrogels in pharmaceutical formulations. *European Journal of Pharmaceutics and Biopharmaceutics* **2000,** *50* (1), 27-46.

22. Whitesides, G.; Mathias, J.; Seto, C., Molecular self-assembly and nanochemistry: a chemical strategy for the synthesis of nanostructures. *Science* **1991,** *254* (5036), 1312-1319.

23. Zhang, S.; Holmes, T.; Lockshin, C.; Rich, A., Spontaneous assembly of a self-complementary oligopeptide to form a stable macroscopic membrane. *Proceedings of the National Academy of Sciences of the United States of America* **1993,** *90* (8), 3334-3338.

24. Narayanaswamy, R.; Torchilin, V. P., Hydrogels and Their Applications in Targeted Drug Delivery. *Molecules (Basel, Switzerland)* **2019,** *24* (3), 603.

25. Urry, D. W.; Pattanaik, A., Elastic Protein-based Materials in Tissue Reconstructiona. *Annals of the New York Academy of Sciences* **1997,** *831* (1), 32-46.

26. (a) Hwang, J. J.; Iyer, S. N.; Li, L.-S.; Claussen, R.; Harrington, D. A.; Stupp, S. I., Self-assembling biomaterials: Liquid crystal phases of cholesteryl oligo(l-lactic acid) and their interactions with cells. *Proceedings of the National Academy of Sciences* **2002,** *99* (15), 9662-9667; (b) Cui, H.; Webber, M. J.; Stupp, S. I., Self-assembly of peptide amphiphiles: From molecules to nanostructures to biomaterials. *Peptide Science* **2010,** *94* (1), 1-18.

27. Schloss, A. C.; Williams, D. M.; Regan, L. J., Protein-Based Hydrogels for Tissue Engineering. *Advances in experimental medicine and biology* **2016,** *940*, 167-177.

28. Zhang, S., Emerging biological materials through molecular self-assembly. *Biotechnology Advances* **2002,** *20* (5), 321-339.

29. Pauling, L., *The Nature of the Chemical Bond*. 3 ed.; Cornell University Press: Ithaca NY, 1960; Vol. 1, p 644.

30. Ozbas, B.; Kretsinger, J.; Rajagopal, K.; Schneider, J. P.; Pochan, D. J., Salt-Triggered Peptide Folding and Consequent Self-Assembly into Hydrogels with Tunable Modulus. *Macromolecules* **2004,** *37* (19), 7331-7337.

31. Banwell, E. F.; Abelardo, E. S.; Adams, D. J.; Birchall, M. A.; Corrigan, A.; Donald, A. M.; Kirkland, M.; Serpell, L. C.; Butler, M. F.; Woolfson, D. N., Rational design and application of responsive α-helical peptide hydrogels. *Nature Materials* **2009,** *8*, 596.

32. Geckil, H.; Xu, F.; Zhang, X.; Moon, S.; Demirci, U., Engineering hydrogels as extracellular matrix mimics. *Nanomedicine (London, England)* **2010,** *5* (3), 469-484.

33. Naahidi, S.; Jafari, M.; Logan, M.; Wang, Y.; Yuan, Y.; Bae, H.; Dixon, B.; Chen, P., Biocompatibility of hydrogel-based scaffolds for tissue engineering applications. *Biotechnology Advances* **2017,** *35* (5), 530-544.

34. Lu, Y.; Sun, W.; Gu, Z., Stimuli-responsive nanomaterials for therapeutic protein delivery. *Journal of Controlled Release* **2014,** *194*, 1-19.

35. Jonker, A. M.; Löwik, D. W. P. M.; van Hest, J. C. M., Peptide- and Protein-Based Hydrogels. *Chemistry of Materials* **2012,** *24* (5), 759-773.

36. Yan, H.; Saiani, A.; Gough, J. E.; Miller, A. F., Thermoreversible Protein Hydrogel as Cell Scaffold. *Biomacromolecules* **2006,** *7* (10), 2776-2782.

37. (a) Kamoun, E. A.; Kenawy, E.-R. S.; Chen, X., A review on polymeric hydrogel membranes for wound dressing applications: PVA-based hydrogel dressings. *Journal of Advanced Research* **2017,** *8* (3), 217-233; (b) Zhao, X.; Wu, H.; Guo, B.; Dong, R.; Qiu, Y.; Ma, P. X., Antibacterial anti-oxidant electroactive injectable hydrogel as self-healing wound dressing with hemostasis and adhesiveness for cutaneous wound healing. *Biomaterials* **2017,** *122*, 34-47; (c) Chin, S. Y.; Poh, Y. C.; Kohler, A.-C.; Compton, J. T.; Hsu, L. L.; Lau, K. M.; Kim, S.; Lee, B. W.; Lee, F. Y.; Sia, S. K., Additive manufacturing of hydrogel-based materials for next-generation implantable medical devices. *Science Robotics* **2017,** *2* (2).

38. (a) Pollard, T. D.; Cooper, J. A., Actin and actin-binding proteins. A critical evaluation of mechanisms and functions. *Annual review of biochemistry* **1986,** *55* (1), 987-1035; (b) Dominguez, R.; Holmes, K. C., Actin structure and function. *Annual review of biophysics* **2011,** *40*, 169-186.

39. Lieleg, O.; Claessens, M. M. A. E.; Bausch, A. R., Structure and dynamics of cross-linked actin networks. *Soft Matter* **2010,** *6* (2), 218-225.

40. Lieleg, O.; Claessens, M. M. A. E.; Luan, Y.; Bausch, A. R., Transient Binding and Dissipation in Cross-Linked Actin Networks. *Physical Review Letters* **2008,** *101* (10), 108101.

41. Indermun, S.; Govender, M.; Kumar, P.; Choonara, Y. E.; Pillay, V., 2 - Stimuli-responsive polymers as smart drug delivery systems: Classifications based on carrier type and triggered-release mechanism. In *Stimuli Responsive Polymeric Nanocarriers for Drug Delivery Applications, Volume 1*, Makhlouf, A. S. H.; Abu-Thabit, N. Y., Eds. Woodhead Publishing: 2018; pp 43-58.

42. (a) Overstreet, D. J.; McLemore, R. Y.; Doan, B. D.; Farag, A.; Vernon, B. L., Temperature-Responsive Graft Copolymer Hydrogels for Controlled Swelling and Drug Delivery. *Soft Materials* **2013,**

11 (3), 294-304; (b) Schoener, C. A.; Hutson, H. N.; Peppas, N. A., pH-responsive hydrogels with dispersed hydrophobic nanoparticles for the oral delivery of chemotherapeutics. *Journal of Biomedical Materials Research Part A* **2012,** *101A* (8), 2229-2236; (c) Xu, Y.; Ghag, O.; Reimann, M.; Sitterle, P.; Chatterjee, P.; Nofen, E.; Yu, H.; Jiang, H.; Dai, L. L., Development of visible-light responsive and mechanically enhanced "smart" UCST interpenetrating network hydrogels. *Soft matter* **2018,** *14* (1), 151-160; (d) Culver, H. R.; Clegg, J. R.; Peppas, N. A., Analyte-Responsive Hydrogels: Intelligent Materials for Biosensing and Drug Delivery. *Accounts of Chemical Research* **2017,** *50* (2), 170-178.

43. Urry, D. W.; Urry, K. D.; Szaflarski, W.; Nowicki, M., Elastic-contractile model proteins: Physical chemistry, protein function and drug design and delivery. *Advanced Drug Delivery Reviews* **2010,** *62* (15), 1404-1455.

44. Holmes, K. C., Actin in a twist. *Nature* **2009,** *457*, 389.

45. Mornet, D.; Ue, K., Proteolysis and structure of skeletal muscle actin. *Proceedings of the National Academy of Sciences* **1984,** *81* (12), 3680-3684.

46. (a) Spracklen, A. J.; Fagan, T. N.; Lovander, K. E.; Tootle, T. L., The pros and cons of common actin labeling tools for visualizing actin dynamics during Drosophila oogenesis. *Developmental Biology* **2014,** *393* (2), 209-226; (b) Ishimoto, T.; Ozawa, T.; Mori, H., Real-Time Monitoring of Actin Polymerization in Living Cells Using Split Luciferase. *Bioconjugate Chemistry* **2011,** *22* (6), 1136-1144.

47. Sano, K.-I.; Kawamura, R.; Tominaga, T.; Oda, N.; Ijiro, K.; Osada, Y., Self-Repairing Filamentous Actin Hydrogel with Hierarchical Structure. *Biomacromolecules* **2011,** *12* (12), 4173-4177.

48. Chivers, C. E.; Koner, A. L.; Lowe, E. D.; Howarth, M., How the biotin-streptavidin interaction was made even stronger: investigation via crystallography and a chimaeric tetramer. *The Biochemical journal* **2011,** *435* (1), 55-63.

49. (a) Sajja, S.; Roark Brandon, K.; Chandler, M.; Jones, M., Blink and you'll miss it: a new biosensing strategy with nucleic acids. In *DNA and RNA Nanotechnology*, 2017; Vol. 4, p 21; (b) Roark, B.; Tan, J. A.; Ivanina, A.; Chandler, M.; Castaneda, J.; Kim, H. S.; Jawahar, S.; Viard, M.; Talic, S.; Wustholz, K. L.; Yingling, Y. G.; Jones, M.; Afonin, K. A., Fluorescence Blinking as an Output Signal for Biosensing. *ACS sensors* **2016,** *1* (11), 1295-1300.

50. Zhang, N.; Ma, P.; Xu, S.; Fan, A.; Zhao, Y.; Xue, W.; Luo, Y.; Fan, H., Research advances and applications of nucleic acid-modified techniques for biomedical nanomaterial. *Journal of Alloys and Compounds* **2018,** *742*, 629-640.

51. (a) Liu, S.; Su, W.; Li, Y.; Zhang, L.; Ding, X., Manufacturing of an electrochemical biosensing platform based on hybrid DNA hydrogel: Taking lung cancer-specific miR-21 as an example. *Biosensors and Bioelectronics* **2018,** *103*, 1-5; (b) Mao, X.; Chen, G.; Wang, Z.; Zhang, Y.; Zhu, X.; Li, G., Surface-immobilized and self-shaped DNA hydrogels and their application in biosensing. *Chemical Science* **2018,** *9* (4), 811-818.

52. Li, J.; Mooney, D. J., Designing hydrogels for controlled drug delivery. *Nature reviews. Materials* **2016,** *1* (12), 16071.

53. Zhu, J.; Marchant, R. E., Design properties of hydrogel tissue-engineering scaffolds. *Expert review of medical devices* **2011,** *8* (5), 607-626.

54. Song, J.; Im, K.; Hwang, S.; Hur, J.; Nam, J.; Ahn, G. O.; Hwang, S.; Kim, S.; Park, N., DNA hydrogel delivery vehicle for light-triggered and synergistic cancer therapy. *Nanoscale* **2015,** *7* (21), 9433-9437.

55. Seeman, N. C.; Sussman, J. L.; Berman, H. N.; Kim, S. H., Nucleic acid conformation: crystal structure of a naturally occurring dinucleoside phosphate (UpA). *Nat New Biol* **1971,** *233* (37), 90-92.

56. Seeman, N. C.; Kallenbach, N. R., Design of immobile nucleic acid junctions. *Biophysical journal* **1983,** *44* (2), 201-209.

57. Cohen, S. N.; Chang, A. C.; Boyer, H. W.; Helling, R. B., Construction of biologically functional bacterial plasmids in vitro. *Proceedings of the National Academy of Sciences of the United States of America* **1973,** *70* (11), 3240-3244.

58. Seeman, N. C., Nucleic acid junctions and lattices. *Journal of Theoretical Biology* **1982,** *99* (2), 237-247.

59. Shen, Z.; Yan, H.; Wang, T.; Seeman, N. C., Paranemic Crossover DNA: A Generalized Holliday Structure with Applications in Nanotechnology. *Journal of the American Chemical Society* **2004,** *126* (6), 1666-1674.

60. (a) Shih, W. M.; Quispe, J. D.; Joyce, G. F., A 1.7-kilobase single-stranded DNA that folds into a nanoscale octahedron. *Nature* **2004,** *427* (6975), 618-621; (b) Zhang, X.; Yan, H.; Shen, Z.; Seeman, N. C., Paranemic Cohesion of Topologically-Closed DNA Molecules. *Journal of the American Chemical Society* **2002,** *124* (44), 12940-12941; (c) Kuzuya, A.; Wang, R.; Sha, R.; Seeman, N. C., Six-Helix and Eight-Helix DNA Nanotubes Assembled from Half-Tubes. *Nano Letters* **2007,** *7* (6), 1757-1763.

61. Rothemund, P. W., Folding DNA to create nanoscale shapes and patterns. *Nature* **2006,** *440* (7082), 297-302.

62. (a) Andersen, E. S.; Dong, M.; Nielsen, M. M.; Jahn, K.; Lind-Thomsen, A.; Mamdouh, W.; Gothelf, K. V.; Besenbacher, F.; Kjems, J., DNA origami design of dolphin-shaped structures with flexible tails. *ACS Nano* **2008,** *2* (6), 1213-8; (b) Ke, Y.; Sharma, J.; Liu, M.; Jahn, K.; Liu, Y.; Yan, H., Scaffolded DNA origami of a DNA tetrahedron molecular container. *Nano Lett* **2009,** *9* (6), 2445-7; (c) Andersen, E. S.; Dong, M.; Nielsen, M. M.; Jahn, K.; Subramani, R.; Mamdouh, W.; Golas, M. M.; Sander, B.; Stark, H.; Oliveira, C. L. P.; Pedersen, J. S.; Birkedal, V.; Besenbacher, F.; Gothelf, K. V.; Kjems, J., Self-assembly of a nanoscale DNA box with a controllable lid. *Nature* **2009,** *459*, 73; (d) Dietz, H.; Douglas, S. M.; Shih, W. M., Folding DNA into twisted and curved nanoscale shapes. *Science (New York, N.Y.)* **2009,** *325* (5941), 725-730.

63. (a) Guo, P., The emerging field of RNA nanotechnology. *Nature nanotechnology* **2010,** *5* (12), 833-842; (b) Chworos, A.; Severcan, I.; Koyfman, A. Y.; Weinkam, P.; Oroudjev, E.; Hansma, H. G.; Jaeger, L., Building Programmable Jigsaw Puzzles with RNA. *Science* **2004,** *306* (5704), 2068.

64. Leontis, N. B.; Lescoute, A.; Westhof, E., The building blocks and motifs of RNA architecture. *Current opinion in structural biology* **2006,** *16* (3), 279-287.

65. (a) Seshachar, B. R.; Dass, C. M. S., Evidence for the conversion of desoxyribonucleic acid (DNA) to ribonucleic acid (RNA) in Epistylis articulata from. (Ciliata: Peritricha). *Experimental Cell Research* **1953,** *5* (1), 248-250; (b) Dounce, A. L., Nucleic Acid Template Hypotheses. *Nature* **1953,** *172* (4377), 541-541; (c) Geiduschek, E. P.; Haselkorn, R., Messenger RNA. *Annual Review of Biochemistry* **1969,** *38* (1), 647-676; (d) Crick, F. H., The origin of the genetic code. *J Mol Biol* **1968,** *38* (3), 367-79.

66. (a) Altman, S.; Baer, M.; Guerrier-Takada, C.; Vioque, A., Enzymatic cleavage of RNA by RNA. *Trends in Biochemical Sciences* **1986,** *11* (12), 515-518; (b) Guerrier-Takada, C.; Gardiner, K.; Marsh, T.; Pace, N.; Altman, S., The RNA moiety of ribonuclease P is the catalytic subunit of the enzyme. *Cell* **1983,** *35* (3 Pt 2), 849-57.

67. (a) Jaeger, L.; Leontis, N. B., Tecto-RNA: One-Dimensional Self-Assembly through Tertiary Interactions. *Angewandte Chemie International Edition* **2000,** *39* (14), 2521-2524; (b) Brion, P.; Westhof, E., HIERARCHY AND DYNAMICS OF RNA FOLDING. *Annual Review of Biophysics and Biomolecular Structure* **1997,** *26* (1), 113-137.

68. Sigler, P. B., An Analysis of the Structure of tRNA. *Annual Review of Biophysics and Bioengineering* **1975,** *4* (1), 477-527.

69. Leontis, N. B.; Stombaugh, J.; Westhof, E., The non-Watson-Crick base pairs and their associated isostericity matrices. *Nucleic Acids Res* **2002,** *30* (16), 3497-531.

70. Jaeger, L.; Westhof, E.; Leontis, N. B., TectoRNA: modular assembly units for the construction of RNA nano-objects. *Nucleic Acids Research* **2001,** *29* (2), 455-463.

71. (a) Zhang, H.; Endrizzi, J. A.; Shu, Y.; Haque, F.; Sauter, C.; Shlyakhtenko, L. S.; Lyubchenko, Y.; Guo, P.; Chi, Y. I., Crystal structure of 3WJ core revealing divalent ion-promoted thermostability and assembly of the Phi29 hexameric motor pRNA. *RNA (New York, N.Y.)* **2013,** *19* (9), 1226-37; (b) Shu, D.; Khisamutdinov, E. F.; Zhang, L.; Guo, P., Programmable folding of fusion RNA in vivo and in vitro driven by pRNA 3WJ motif of phi29 DNA packaging motor. *Nucleic Acids Res* **2014,** *42* (2), e10; (c) Guo, P.; Zhang, C.; Chen, C.; Garver, K.; Trottier, M., Inter-RNA interaction of phage phi29 pRNA to form a hexameric complex for viral DNA transportation. *Molecular cell* **1998,** *2* (1), 149-155.

72. Khisamutdinov, E. F.; Bui, M. N.; Jasinski, D.; Zhao, Z.; Cui, Z.; Guo, P., Simple Method for Constructing RNA Triangle, Square, Pentagon by Tuning Interior RNA 3WJ Angle from 60 degrees to 90 degrees or 108 degrees. *Methods in molecular biology (Clifton, N.J.)* **2015,** *1316*, 181-93.

73. Yingling, Y. G.; Shapiro, B. A., Computational Design of an RNA Hexagonal Nanoring and an RNA Nanotube. *Nano Letters* **2007,** *7* (8), 2328-2334.

74. Shu, D.; Moll, W.-D.; Deng, Z.; Mao, C.; Guo, P., Bottom-up Assembly of RNA Arrays and Superstructures as Potential Parts in Nanotechnology. *Nano letters* **2004,** *4* (9), 1717-1723.

75. (a) Pley, H. W.; Flaherty, K. M.; McKay, D. B., Three-dimensional structure of a hammerhead ribozyme. *Nature* **1994,** *372* (6501), 68-74; (b) Scott, W. G.; Horan, L. H.; Martick, M., The hammerhead ribozyme: structure, catalysis, and gene regulation. *Progress in molecular biology and translational science* **2013,** *120*, 1-23.

76. (a) Bechtel, J. M.; Rajesh, P.; Ilikchyan, I.; Deng, Y.; Mishra, P. K.; Wang, Q.; Wu, X.; Afonin, K. A.; Grose, W. E.; Wang, Y.; Khuder, S.; Fedorov, A., The Alternative Splicing Mutation Database: a hub for investigations of alternative splicing using mutational evidence. *BMC Res Notes* **2008,** *1*, 3; (b) Bechtel, J. M.; Rajesh, P.; Ilikchyan, I.; Deng, Y.; Mishra, P. K.; Wang, Q.; Wu, X.; Afonin, K. A.; Grose, W. E.; Wang, Y.; Khuder, S.; Fedorov, A., Calculation of splicing potential from the Alternative Splicing Mutation Database. *BMC Res Notes* **2008,** *1*, 4.

77. (a) Huang, L.; Lilley, D. M. J., The Kink Turn, a Key Architectural Element in RNA Structure. *Journal of molecular biology* **2016,** *428* (5 Pt A), 790-801; (b) Afonin, K. A.; Leontis, N. B., Generating new specific RNA interaction interfaces using C-loops. *Journal of the American Chemical Society* **2006,** *128* (50), 16131-16137; (c) Afonin, K. A.; Cieply, D. J.; Leontis, N. B., Specific RNA Self-Assembly with Minimal Paranemic Motifs. *Journal of the American Chemical Society* **2008,** *130* (1), 93-102; (d) Afonin, K. A.; Danilov, E. O.; Novikova, I. V.; Leontis, N. B., TokenRNA: a new type of sequence-specific, label-free fluorescent biosensor for folded RNA molecules. *Chembiochem : a European journal of chemical biology* **2008,** *9* (12), 1902-1905; (e) Afonin, K. A.; Lin, Y.-P.; Calkins, E. R.; Jaeger, L., Attenuation of loop-receptor interactions with pseudoknot formation. *Nucleic acids research* **2012,** *40* (5), 2168-2180; (f) Grabow, W. W.; Zakrevsky, P.; Afonin, K. A.; Chworos, A.; Shapiro, B. A.; Jaeger, L., Self-Assembling RNA Nanorings Based on RNAI/II Inverse Kissing Complexes. *Nano Letters* **2011,** *11* (2), 878-887; (g)

Bindewald, E.; Afonin, K.; Jaeger, L.; Shapiro, B. A., Multistrand RNA secondary structure prediction and nanostructure design including pseudoknots. *ACS nano* **2011,** *5* (12), 9542-9551.

78. (a) R Breaker, R., *Breaker, R.R. Engineered allosteric ribozymes as biosensor components. Curr. Opin. Biotechnol. 13, 31-39*. 2002; Vol. 13, p 31-9; (b) Jaschke, A., Artificial ribozymes and deoxyribozymes. *Curr Opin Struct Biol* **2001,** *11* (3), 321-6; (c) Nimjee, S. M.; Rusconi, C. P.; Sullenger, B. A., Aptamers: an emerging class of therapeutics. *Annual review of medicine* **2005,** *56*, 555-83; (d) Xiao, Z.; Farokhzad, O. C., Aptamer-functionalized nanoparticles for medical applications: challenges and opportunities. *ACS nano* **2012,** *6* (5), 3670-3676; (e) Thiel, K. W.; Giangrande, P. H., Therapeutic applications of DNA and RNA aptamers. *Oligonucleotides* **2009,** *19* (3), 209-22; (f) Tucker, B. J.; Breaker, R. R., Riboswitches as versatile gene control elements. *Curr Opin Struct Biol* **2005,** *15* (3), 342-8; (g) Pecot, C. V.; Calin, G. A.; Coleman, R. L.; Lopez-Berestein, G.; Sood, A. K., RNA interference in the clinic: challenges and future directions. *Nature reviews. Cancer* **2011,** *11* (1), 59-67; (h) Petrocca, F.; Lieberman, J., Promise and challenge of RNA interference-based therapy for cancer. *Journal of clinical oncology : official journal of the American Society of Clinical Oncology* **2011,** *29* (6), 747-54; (i) Davis, M. E.; Zuckerman, J. E.; Choi, C. H. J.; Seligson, D.; Tolcher, A.; Alabi, C. A.; Yen, Y.; Heidel, J. D.; Ribas, A., Evidence of RNAi in humans from systemically administered siRNA via targeted nanoparticles. *Nature* **2010,** *464*, 1067.

79. (a) Bernstein, E.; Caudy, A. A.; Hammond, S. M.; Hannon, G. J., Role for a bidentate ribonuclease in the initiation step of RNA interference. *Nature* **2001,** *409* (6818), 363-366; (b) Wassenegger, M.; Pelissier, T., A model for RNA-mediated gene silencing in higher plants. *Plant molecular biology* **1998,** *37* (2), 349-62; (c) Sharp, P. A., RNAi and double-strand RNA. *Genes & Development* **1999,** *13* (2), 139-141; (d) Siomi, H.; Siomi, M. C., On the road to reading the RNA-interference code. *Nature* **2009,** *457*, 396.

80. (a) Afonin, K. A.; Kasprzak, W. K.; Bindewald, E.; Kireeva, M.; Viard, M.; Kashlev, M.; Shapiro, B. A., In silico design and enzymatic synthesis of functional RNA nanoparticles. *Accounts of chemical research* **2014,** *47* (6), 1731-1741; (b) Afonin, K. A.; Bindewald, E.; Yaghoubian, A. J.; Voss, N.; Jacovetty, E.; Shapiro, B. A.; Jaeger, L., In vitro assembly of cubic RNA-based scaffolds designed in silico. *Nature Nanotechnology* **2010,** *5*, 676; (c) Bindewald, E.; Grunewald, C.; Boyle, B.; O'Connor, M.; Shapiro, B. A., Computational strategies for the automated design of RNA nanoscale structures from building blocks using NanoTiler. *Journal of molecular graphics & modelling* **2008,** *27* (3), 299-308.

81. (a) Cornell, W. D.; Cieplak, P.; Bayly, C. I.; Gould, I. R.; Merz, K. M.; Ferguson, D. M.; Spellmeyer, D. C.; Fox, T.; Caldwell, J. W.; Kollman, P. A., A Second Generation Force Field for the Simulation of Proteins, Nucleic Acids, and Organic Molecules. *Journal of the American Chemical Society* **1995,** *117* (19), 5179-5197; (b) Hanwell, M. D.; Curtis, D. E.; Lonie, D. C.; Vandermeersch, T.; Zurek, E.; Hutchison, G. R., Avogadro: an advanced semantic chemical editor, visualization, and analysis platform. *Journal of Cheminformatics* **2012,** *4* (1), 17; (c) Brooks, B. R.; Brooks, C. L., 3rd; Mackerell, A. D., Jr.; Nilsson, L.; Petrella, R. J.; Roux, B.; Won, Y.; Archontis, G.; Bartels, C.; Boresch, S.; Caflisch, A.; Caves, L.; Cui, Q.; Dinner, A. R.; Feig, M.; Fischer, S.; Gao, J.; Hodoscek, M.; Im, W.; Kuczera, K.; Lazaridis, T.; Ma, J.; Ovchinnikov, V.; Paci, E.; Pastor, R. W.; Post, C. B.; Pu, J. Z.; Schaefer, M.; Tidor, B.; Venable, R. M.; Woodcock, H. L.; Wu, X.; Yang, W.; York, D. M.; Karplus, M., CHARMM: the biomolecular simulation program. *Journal of computational chemistry* **2009,** *30* (10), 1545-614; (d) Eswar, N.; Webb, B.; Marti-Renom, M. A.; Madhusudhan, M. S.; Eramian, D.; Shen, M. Y.; Pieper, U.; Sali, A., Comparative protein structure modeling using MODELLER. *Current protocols in protein science* **2007,** *Chapter 2*, Unit 2.9; (e) Rocchia, W.; Alexov, E.; Honig, B., Extending the Applicability of the Nonlinear Poisson−Boltzmann Equation: Multiple Dielectric Constants and Multivalent Ions. *The Journal of Physical Chemistry B* **2001,** *105* (28), 6507-6514; (f) Chen, R.; Li, L.; Weng, Z., ZDOCK: an initial-stage protein-docking algorithm. *Proteins* **2003,** *52* (1), 80-7; (g) Lyubartsev, A. P.; Laaksonen, A., M.DynaMix – a scalable portable parallel MD simulation package for arbitrary molecular mixtures. *Computer Physics Communications* **2000,** *128* (3), 565-589.

82. Johnson, M. B.; Halman, J. R.; Satterwhite, E.; Zakharov, A. V.; Bui, M. N.; Benkato, K.; Goldsworthy, V.; Kim, T.; Hong, E.; Dobrovolskaia, M. A.; Khisamutdinov, E. F.; Marriott, I.; Afonin, K.

A., Programmable Nucleic Acid Based Polygons with Controlled Neuroimmunomodulatory Properties for Predictive QSAR Modeling. *Small* **2017,** *13* (42), 1701255.

83. Afonin, K. A.; Viard, M.; Kagiampakis, I.; Case, C. L.; Dobrovolskaia, M. A.; Hofmann, J.; Vrzak, A.; Kireeva, M.; Kasprzak, W. K.; KewalRamani, V. N.; Shapiro, B. A., Triggering of RNA interference with RNA-RNA, RNA-DNA, and DNA-RNA nanoparticles. *ACS nano* **2015,** *9* (1), 251-259.

84. Li, J.; Mo, L.; Lu, C.-H.; Fu, T.; Yang, H.-H.; Tan, W., Functional nucleic acid-based hydrogels for bioanalytical and biomedical applications. *Chemical Society reviews* **2016,** *45* (5), 1410-1431.

85. Zuker, M., Mfold web server for nucleic acid folding and hybridization prediction. *Nucleic acids research* **2003,** *31* (13), 3406-3415.

86. (a) Afonin, K. A.; Kasprzak, W.; Bindewald, E.; Puppala, P. S.; Diehl, A. R.; Hall, K. T.; Kim, T. J.; Zimmermann, M. T.; Jernigan, R. L.; Jaeger, L.; Shapiro, B. A., Computational and experimental characterization of RNA cubic nanoscaffolds. *Methods (San Diego, Calif.)* **2014,** *67* (2), 256-265; (b) Computational and Experimental RNA Nanoparticle Design. In *Automation in Proteomics and Genomics*.

87. Rose, S. D.; Kim, D. H.; Amarzguioui, M.; Heidel, J. D.; Collingwood, M. A.; Davis, M. E.; Rossi, J. J.; Behlke, M. A., Functional polarity is introduced by Dicer processing of short substrate RNAs. *Nucleic Acids Res* **2005,** *33* (13), 4140-56.

88. (a) Afonin, K. A.; Grabow, W. W.; Walker, F. M.; Bindewald, E.; Dobrovolskaia, M. A.; Shapiro, B. A.; Jaeger, L., Design and self-assembly of siRNA-functionalized RNA nanoparticles for use in automated nanomedicine. *Nat Protoc* **2011,** *6* (12), 2022-34; (b) Afonin, K. A.; Viard, M.; Tedbury, P.; Bindewald, E.; Parlea, L.; Howington, M.; Valdman, M.; Johns-Boehme, A.; Brainerd, C.; Freed, E. O.; Shapiro, B. A., The Use of Minimal RNA Toeholds to Trigger the Activation of Multiple Functionalities. *Nano letters* **2016,** *16* (3), 1746-53; (c) Stewart, J. M.; Viard, M.; Subramanian, H. K.; Roark, B. K.; Afonin, K. A.; Franco, E., Programmable RNA microstructures for coordinated delivery of siRNAs. *Nanoscale* **2016,** *8* (40), 17542-17550; (d) Bui, M. N.; Brittany Johnson, M.; Viard, M.; Satterwhite, E.; Martins, A. N.; Li, Z.; Marriott, I.; Afonin, K. A.; Khisamutdinov, E. F., Versatile RNA tetra-U helix linking motif as a toolkit for nucleic acid nanotechnology. *Nanomedicine* **2017,** *13* (3), 1137-1146.

89. Afonin, K. A.; Kireeva, M.; Grabow, W. W.; Kashlev, M.; Jaeger, L.; Shapiro, B. A., Co-transcriptional assembly of chemically modified RNA nanoparticles functionalized with siRNAs. *Nano letters* **2012,** *12* (10), 5192-5.

90. (a) Liu, Y. P.; von Eije, K. J.; Schopman, N. C.; Westerink, J. T.; ter Brake, O.; Haasnoot, J.; Berkhout, B., Combinatorial RNAi against HIV-1 using extended short hairpin RNAs. *Molecular therapy : the journal of the American Society of Gene Therapy* **2009,** *17* (10), 1712-23; (b) Grimm, D.; Kay, M. A., Combinatorial RNAi: A Winning Strategy for the Race Against Evolving Targets? *Molecular Therapy* **2007,** *15* (5), 878-888; (c) Afonin, K. A.; Viard, M.; Koyfman, A. Y.; Martins, A. N.; Kasprzak, W. K.; Panigaj, M.; Desai, R.; Santhanam, A.; Grabow, W. W.; Jaeger, L.; Heldman, E.; Reiser, J.; Chiu, W.; Freed, E. O.; Shapiro, B. A., Multifunctional RNA Nanoparticles. *Nano Letters* **2014,** *14* (10), 5662-5671.

91. Sajja, S.; Chandler, M.; Fedorov, D.; Kasprzak, W. K.; Lushnikov, A.; Viard, M.; Shah, A.; Dang, D.; Dahl, J.; Worku, B.; Dobrovolskaia, M. A.; Krasnoslobodtsev, A.; Shapiro, B. A.; Afonin, K. A., Dynamic Behavior of RNA Nanoparticles Analyzed by AFM on a Mica/Air Interface. *Langmuir* **2018,** *34* (49), 15099-15108.

92. (a) Gurcan, M. N.; Boucheron, L. E.; Can, A.; Madabhushi, A.; Rajpoot, N. M.; Yener, B., Histopathological Image Analysis: A Review. *IEEE Reviews in Biomedical Engineering* **2009,** *2*, 147-171; (b) Klapetek, P.; Valtr, M.; Nečas, D.; Salyk, O.; Dzik, P., Atomic force microscopy analysis of nanoparticles in non-ideal conditions. *Nanoscale Research Letters* **2011,** *6* (1), 514.

93. Cangialosi, A.; Yoon, C.; Liu, J.; Huang, Q.; Guo, J.; Nguyen, T. D.; Gracias, D. H.; Schulman, R., DNA sequence–directed shape change of photopatterned hydrogels via high-degree swelling. *Science* **2017,** *357* (6356), 1126.

94. Stephanopoulos, N.; Francis, M. B., Choosing an effective protein bioconjugation strategy. *Nature Chemical Biology* **2011,** *7*, 876.

95. Boutureira, O.; Bernardes, G. J. L., Advances in Chemical Protein Modification. *Chemical Reviews* **2015,** *115* (5), 2174-2195.

96. Collins, J. H.; Elzinga, M., The primary structure of actin from rabbit skeletal muscle. Completion and analysis of the amino acid sequence. *Journal of Biological Chemistry* **1975,** *250* (15), 5915-5920.

97. Ji, J.; Chakraborty, A.; Geng, M.; Zhang, X.; Amini, A.; Bina, M.; Regnier, F., Strategy for qualitative and quantitative analysis in proteomics based on signature peptides. *Journal of Chromatography B: Biomedical Sciences and Applications* **2000,** *745* (1), 197-210.

98. Alegria-Schaffer, A., Chapter Six - General Protein–Protein Cross-Linking. In *Methods in Enzymology*, Lorsch, J., Ed. Academic Press: 2014; Vol. 539, pp 81-87.

99. Fessler, A. B.; Dey, A.; Garmon, C. B.; Finis, D. S.; Saleh, N.-A.; Fowler, A. J.; Jones, D. S.; Chakrabarti, K.; Ogle, C. A., Water-Soluble Isatoic Anhydrides: A Platform for RNA-SHAPE Analysis and Protein Bioconjugation. *Bioconjugate Chemistry* **2018,** *29* (9), 3196-3202.

100. (a) Chalfie, M., GFP: Lighting up life. *Proceedings of the National Academy of Sciences of the United States of America* **2009,** *106* (25), 10073-10080; (b) Chalfie, M.; Tu, Y.; Euskirchen, G.; Ward, W. W.; Prasher, D. C., Green fluorescent protein as a marker for gene expression. *Science* **1994,** *263* (5148), 802; (c) Shimomura, O.; Johnson, F. H.; Saiga, Y., Extraction, Purification and Properties of Aequorin, a Bioluminescent Protein from the Luminous Hydromedusan, Aequorea. *Journal of Cellular and Comparative Physiology* **1962,** *59* (3), 223-239; (d) Morise, H.; Shimomura, O.; Johnson, F. H.; Winant, J., Intermolecular energy transfer in the bioluminescent system of Aequorea. *Biochemistry* **1974,** *13* (12), 2656-2662.

101. Olesya, V. S.; Vladislav, V. V.; Irina, M. K.; Vladimir, N. U.; Turoverov, K. K., Fluorescent Proteins as Biomarkers and Biosensors: Throwing Color Lights on Molecular and Cellular Processes. *Current Protein & Peptide Science* **2008,** *9* (4), 338-369.

102. Ormö, M.; Cubitt, A. B.; Kallio, K.; Gross, L. A.; Tsien, R. Y.; Remington, S. J., Crystal Structure of the Aequorea victoria Green Fluorescent Protein. *Science* **1996,** *273* (5280), 1392.

103. Soboleski, M. R.; Oaks, J.; Halford, W. P., Green fluorescent protein is a quantitative reporter of gene expression in individual eukaryotic cells. *FASEB journal : official publication of the Federation of American Societies for Experimental Biology* **2005,** *19* (3), 440-442.

104. Heim, R.; Cubitt, A. B.; Tsien, R. Y., Improved green fluorescence. *Nature* **1995,** *373* (6516), 663-664.

105. Pédelacq, J.-D.; Cabantous, S.; Tran, T.; Terwilliger, T. C.; Waldo, G. S., Engineering and characterization of a superfolder green fluorescent protein. *Nature Biotechnology* **2005,** *24*, 79.

106. Cabantous, S.; Terwilliger, T. C.; Waldo, G. S., Protein tagging and detection with engineered self-assembling fragments of green fluorescent protein. *Nature Biotechnology* **2004,** *23*, 102.

107. Bertrand, E.; Chartrand, P.; Schaefer, M.; Shenoy, S. M.; Singer, R. H.; Long, R. M., Localization of ASH1 mRNA Particles in Living Yeast. *Molecular Cell* **1998,** *2* (4), 437-445.

108. Schwarz-Schilling, M.; Dupin, A.; Chizzolini, F.; Krishnan, S.; Mansy, S. S.; Simmel, F. C., Optimized Assembly of a Multifunctional RNA-Protein Nanostructure in a Cell-Free Gene Expression System. *Nano Letters* **2018,** *18* (4), 2650-2657.

109. Ivanina, A.; Roark, B.; Satterwhite, E.; Halman, J. R.; Chandler, M.; Afonin, K. A.; Shapiro, B. A.; Lu, J. S.; Miller, J.; Viard, M.; Bindewald, E.; Kasprzak, W. K.; Panigaj, M.; Khisamutdinov, E. F.; Bui, M. N.; Dobrovolskaia, M. A., Functionally-interdependent shape-switching nanoparticles with controllable properties. *Nucleic Acids Research* **2017,** *45* (4), 2210-2220.

110. Afonin, K. A.; Viard, M.; Martins, A. N.; Lockett, S. J.; Maciag, A. E.; Freed, E. O.; Heldman, E.; Jaeger, L.; Blumenthal, R.; Shapiro, B. A., Activation of different split functionalities on re-association of RNA-DNA hybrids. *Nature nanotechnology* **2013,** *8* (4), 296-304.

111. Rackley, L.; Stewart, J. M.; Salotti, J.; Krokhotin, A.; Shah, A.; Halman, J. R.; Juneja, R.; Smollett, J.; Lee, L.; Roark, K.; Viard, M.; Tarannum, M.; Vivero-Escoto, J.; Johnson, P. F.; Dobrovolskaia, M. A.; Dokholyan, N. V.; Franco, E.; Afonin, K. A., RNA Fibers as Optimized Nanoscaffolds for siRNA Coordination and Reduced Immunological Recognition. *Advanced Functional Materials* **2018,** *28* (48), 1805959.

112. Ouellet, J., RNA Fluorescence with Light-Up Aptamers. *Frontiers in chemistry* **2016,** *4*, 29-29.

113. (a) Ellington, A. D.; Szostak, J. W., In vitro selection of RNA molecules that bind specific ligands. *Nature* **1990,** *346* (6287), 818-822; (b) Tuerk, C.; Gold, L., Systematic evolution of ligands by exponential enrichment: RNA ligands to bacteriophage T4 DNA polymerase. *Science* **1990,** *249* (4968), 505; (c) Levine, H. A.; Nilsen-Hamilton, M., A mathematical analysis of SELEX. *Computational Biology and Chemistry* **2007,** *31* (1), 11-35.

114. Kolpashchikov, D. M., Binary Malachite Green Aptamer for Fluorescent Detection of Nucleic Acids. *Journal of the American Chemical Society* **2005,** *127* (36), 12442-12443.

115. Stojanovic, M. N.; Kolpashchikov, D. M., Modular Aptameric Sensors. *Journal of the American Chemical Society* **2004,** *126* (30), 9266-9270.

116. Afonin, K. A.; Desai, R.; Viard, M.; Kireeva, M. L.; Bindewald, E.; Case, C. L.; Maciag, A. E.; Kasprzak, W. K.; Kim, T.; Sappe, A.; Stepler, M.; Kewalramani, V. N.; Kashlev, M.; Blumenthal, R.; Shapiro, B. A., Co-transcriptional production of RNA-DNA hybrids for simultaneous release of multiple split functionalities. *Nucleic acids research* **2014,** *42* (3), 2085-2097.

117. (a) Paige, J. S.; Wu, K. Y.; Jaffrey, S. R., RNA Mimics of Green Fluorescent Protein. *Science* **2011,** *333* (6042), 642; (b) Paige, J. S.; Nguyen-Duc, T.; Song, W.; Jaffrey, S. R., Fluorescence imaging of cellular metabolites with RNA. *Science (New York, N.Y.)* **2012,** *335* (6073), 1194-1194.

118. Strack, R. L.; Disney, M. D.; Jaffrey, S. R., A superfolding Spinach2 reveals the dynamic nature of trinucleotide repeat-containing RNA. *Nature methods* **2013,** *10* (12), 1219-1224.

119. (a) Filonov, G. S.; Moon, J. D.; Svensen, N.; Jaffrey, S. R., Broccoli: rapid selection of an RNA mimic of green fluorescent protein by fluorescence-based selection and directed evolution. *Journal of the American Chemical Society* **2014,** *136* (46), 16299-16308; (b) Warner, K. D.; Chen, M. C.; Song, W.; Strack, R. L.; Thorn, A.; Jaffrey, S. R.; Ferré-D'Amaré, A. R., Structural basis for activity of highly efficient RNA mimics of green fluorescent protein. *Nature structural & molecular biology* **2014,** *21* (8), 658-663.

120. (a) Song, W.; Strack, R. L.; Jaffrey, S. R., Imaging bacterial protein expression using genetically encoded RNA sensors. *Nature methods* **2013,** *10* (9), 873-875; (b) Song, W.; Strack, R. L.; Svensen, N.; Jaffrey, S. R., Plug-and-play fluorophores extend the spectral properties of Spinach. *Journal of the American Chemical Society* **2014,** *136* (4), 1198-1201; (c) Filonov, G. S.; Kam, C. W.; Song, W.; Jaffrey, S. R., In-gel imaging of RNA processing using broccoli reveals optimal aptamer expression strategies. *Chemistry & biology* **2015,** *22* (5), 649-660.

121. Sajja, S.; Chandler, M.; D. Striplin, C.; Afonin, K., *Activation of Split RNA Aptamers: Experiments Demonstrating the Enzymatic Synthesis of Short RNAs and Their Assembly As Observed by Fluorescent Response*. 2018; Vol. 95.

122. Chandler, M.; Lyalina, T.; Halman, J.; Rackley, L.; Lee, L.; Dang, D.; Ke, W.; Sajja, S.; Woods, S.; Acharya, S.; Baumgarten, E.; Christopher, J.; Elshalia, E.; Hrebien, G.; Kublank, K.; Saleh, S.; Stallings, B.; Tafere, M.; Striplin, C.; Afonin, K. A., Broccoli Fluorets: Split Aptamers as a User-Friendly Fluorescent Toolkit for Dynamic RNA Nanotechnology. *Molecules (Basel, Switzerland)* **2018,** *23* (12), 3178.

APPENDIX: COMMERCIALLY AVAILABLE MALEIMIDE FUNCTIONALIZED DNA AND SEQUENCES FOR RING AND APTAMER DEVELOPED IN THE PROJECT

Hexameric RNA Nanoparticle Strands

Control RNA nanoring:

nrA
5′-GGGAACC**GUCCACU**GGUUCCCGCUACGAG**AGCCUGC**CUCGUAGC
nrB
5′-GGGAACCGCAGGCUGGUUCCCGCUACGAGAGAACGCCUCGUAGC
nrC
5′-GGGAACCGCGUUCUGGUUCCCGCUACGAGACGUCUCCUCGUAGC
nrD
5′-GGGAACCGAGACGUGGUUCCCGCUACGAGUCGUGGUCUCGUAGC
nrE
5′-GGGAACCACCACGAGGUUCCCGCUACGAGAACCAUCCUCGUAGC
nrF
5′-GGGAACCGAUGGUUGGUUCCCGCUACGAGAGUGGACCUCGUAGC

RNA nanoring with nicks:

nrA_6nts_nicks
5′-ggga**GUCCACU**ucccggcuagAcgag**AGCCUGC**cucgU
nrB_6nts_nicks
5′-gggaGCAGGCUucccggcuagAcgagAGAACGCcucgU
nrC_6nts_nicks
5′-gggaGCGUUCUucccggcuagAcgagACGUCUCcucgU
nrD_6nts_nicks
5′-gggaGAGACGUucccggcuagAcgagUCGUGGUcucgU
nrE_6nts_nicks
5′-gggaACCACGAucccggcuagAcgagAACCAUCcucgU
nrF_6nts_nicks
5′-gggaGAUGGUUucccggcuagAcgagAGUGGACcucgU

Nick for NR
5`-CUAGCC

Broccoli Aptamer Strands

Broccoli:

5′gggaaagUUGCCAUGUGUAUGUGGGAGACGGUCGGGUCCAGAUAUUCGUAUCUGUCGAGUAGA
GUGUGGGCUCCCACAUACUCUGAUGAUCCUUCGGGAUCAUUCAUGGCAA-3′

Broc:

5′-gggaaaUUGCCAUGUGUAUGUGGGAGACGGUCGGGUCCAGAUAUU-3′

Coli:

5′-
gggaaaCGUAUCUGUCGAGUAGAGUGUGGGCUCCCACAUACUCUGAUGAUCCUUCGGGAUCAUU
CAUGGCAA-3′

Actin Experiments and Maleimide functionalized DNA sequences

Materials:
G-Buffer-5 mM MOPS +0.2 mM $CaCl_2$ + .02 mM ATP
F-Buffer-10 mM Tris pH 7.5 + 50 mM KCl + 3 mM $MgCl_2$ + 0.2 mM ATP
DNA Sense 5'-Protected Maleimide-Oligonucleotide strand (Genelink)(5'→ 3')
Mal-GGAGACCGTGACCGGTGGTGCAGATGAACTTCAGGGTCA
DNA Antisense 5'-Protected Maleimide Oligonucleotide strand (Genelink) (5' → 3')
Mal-TGACCCTGAAGTTCATCTGCACCACCGGTCACGGTCTCC

Deprotection Procedure: Oligonucleotides were resuspended in double deionized water and aliquoted, with unused aliquots stored at -20 degrees C. The aliquots needed for the experiment were transferred to pressure rated glass vials. The samples were then freeze dried in a lyophilizer. The dried sample vials were then filled with 1.5 mL of anhydrous toluene with the caps placed on tightly and heated at 95°C for 4 hours. The samples were then placed on a rotoevap at low pressure in a 70°C water bath for 1.5 hours. They were then placed in a vacuum dessicator overnight. Deprotected samples were used within 2 days of deprotection with excess stored in a -20 C freezer. The three goals of the experiment were as follows

Functionalization of actin with 5'-Maleimide functionalized sense and antisense ssDNA strands: Deprotected 5'-Maleimide oligonucleotides were dissolved in [F-Buffer] with G-actin and allowed to react overnight on ice. A 2:1 actin-to-Oligo ratio was used for this experiment- utilizing

216.4 µL of 50 µM oligo per reaction with twice the amount of actin- though this quantity of oligo, as mentioned before, proved to be too high. To combat this, an excess of actin should be used, and the concentration of the oligo should be 5 µM in order to have a sufficient excess concentration of actin.

Purification effectiveness of spin purification vs size cutoff spin column purification for the purpose of separating the unbound oligonucleotide strands from the actin and actin-oligo complex: To compare spin purification to size cutoff spin column purification, the actin-oligonucleotide was purified using both techniques to separate the unbound oligonucleotide from the actin and actin-oligo complex. Spin purification was executed in an ultrafast-centrifuge, spinning each tube – sense and antisense - at 30,000 RPM for two hours and fifteen minutes at 4˚C. The supernatant of both the actin-sense and actin-antisense tubes were collected in order to qualitatively determine the effectiveness of purification. Size cutoff spin column purification was evaluated by mixing 50 µL of actin–oligo complex was mixed with 400 µL of [G-Buffer] and spun in a 30 kDa cutoff column at 14 RCF at 4˚C for two minutes. This was repeated four times. Next, the solution was further diluted according to a 4x dilution scheme by adding [G-buffer] to the 400 µL mark. This was done to lower the concentration of Mg^{2+} in solution to break the functionalized F-actin fibers into their monomeric G-actin components. The solution was diluted first at 4x, then at 16x, and finally at 4x to make a final 256x dilution to lower the Mg^{2+} in solution until the F-actin falls apart and is converted to functionalized G-actin.

Gel Electrophoresis: Two rounds of gel electrophoresis were completed in [40% 37.5:1 Acrylamide:Bis-acrylamide PAGE mini gel (300 V, 150 mA, 20 minutes)]. One gel was run in the presence of 2mM Mg^{2+} - (Figure A1.2) as is standard - while one was run without Mg^{2+} (Figure A1.1).

Both gels were loaded with samples in the same order listed below (From left to right):

1. Sense Strand Control ssDNA
2. Antisense Strand Control ssDNA
3. Flow thru sense byproduct of spin column purification
4. Flow thru antisense byproduct of spin column purification
5. Supernatant from 30K RPM Sense-actin spin purification
6. Supernatant from 30K RPM Antisense-actin spin purification
7. actin-sense Spin Purification Product
8. actin-antisense Spin Purification Product
9. actin-sense Spin Column (> 30kDa) Product
10. actin-antisense Spin Purification (> 30kDa) Product

1) 1 2 3 4 5 6 7 8 9 10

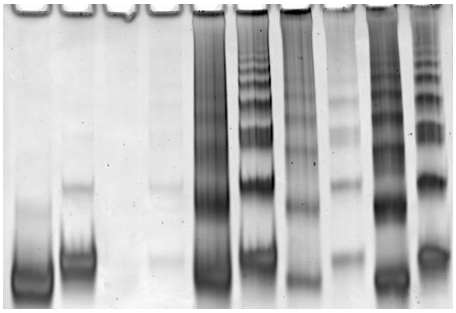

Figure A1.1. PAGE Gel w/o $Mg2^{+}$,

2) 1 2 3 4 5 6 7 8 9 10

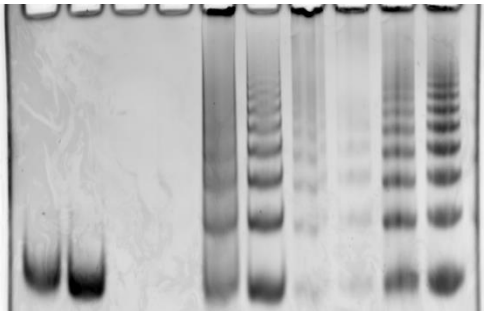

Figure A1.2. PAGE Gel w/$Mg2^{+}$

Discussion: The purpose of this experiment was to determine a superior purification technique, express quantitative data on the binding potential of actin-ssDNA strands and determine the effect of Mg^{2+} in the gel, namely if the presence of Mg^{2+} causes the polymerization of actin. The covalent functionalization of DNA to actin was shown by the marked difference in the bands caused by the control non-functionalized sense and antisense versus the bands shown in the sense-actin and antisense-actin products of both column and spin purification attempts. The presence of multiple bands shows different relative travel distances of labeled G-actin. This is further demonstrated by the lack of bands in the pure non-functionalized actin lane. Since the visualizing agent used was ethidium bromide- which only intercalates DNA- non-labeled actin would not show up and the bands in the actin-sense and actin-antisense would be similar to the control strand lanes. One important minor goal of this experiment was to determine a working purification protocol in order to separate non-functionalized oligonucleotide strands (sense and antisense) and unlabeled actin. This can be observed in the comparison of the supernatant of spin purification vs the flow

thru. The varied bands in the supernatant were indicative of functionalized actin in the supernatant as well as some matching bands to the control sense and antisense lanes. The flow thru lanes show very few unbound strands, possibly due to the excess of actin. This could be further investigated with an excess of sense and antisense strands to measure the level of functionalization (% of bound vs unbound in flow thru). Overall the spin column purification seemed to more effectively purify the actin. However, both purification strategies seemed to leave sense and antisense strands in the actin-strand complex. The Mg^{2+} in the gel did not seem to have any effect on the actin but did show a distinct improvement in gel clarity.

Without Mg^{2+}, the bands seemed smeared and not as clear.

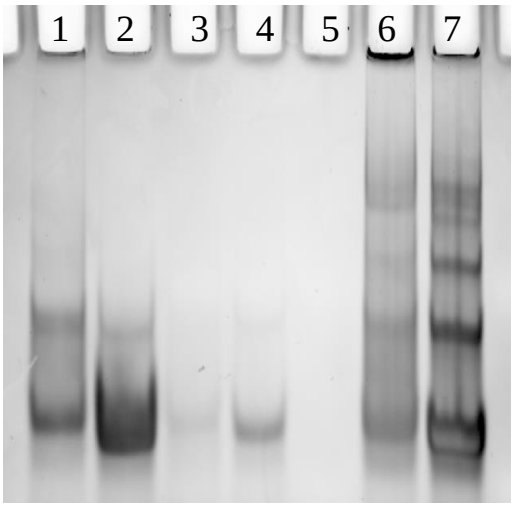

Figure B1.

Legend
1. Sense
2. Antisense
3. Sense Flow Through
4. Antisense Flow Through
5. actin
6. actin – Sense
7. actin – Antisense

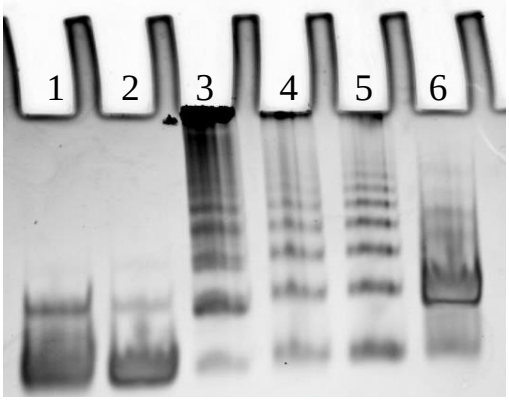

Figure B2.

Legend
1. Sense
2. Antisense
3. G-actin-S-AS-Duplex
4. G-actin-Sense
5. G-actin-Antisense
6. Sense-Antisense

Actin-Duplex Test: This experiment evaluated and compared F-actin fiber formation and actin Duplex fiber formation by first running a Native PAGE Gel with the following scheme: scheme [Native PAGE 37.5.1 – 25 minutes – $Mg2^{+}$ - 5uL sample per well]

Figure B.1 shows preliminary findings that point towards the formation of a DNA S-AS duplex and the actin-S-As-actin Duplex. This can be observed due to the difference in bands between the Sense and AS controls as well as the S-AS duplex. Likewise, the actin duplex exhibited different movement through the gel and aggregated. This follows our guess of it aggregating as it has a 2x higher MW than the single functionalized actin (53 kDa for the non duplex, 106 kDa for the duplex)

Coomassie Blue Gel: This gel was completed according to the following scheme [Native PAGE 37.5.1 – 25 minutes – $Mg2^{+}$ - 5uL sample per well]. This gel was then stained with ethidium bromide for 5 minutes, washed and imaged. The gel was then stained in Coomassie Brilliant Blue dye for one hour before being de-stained for two hours. It was then left in the de-staining solution overnight at 4°C.

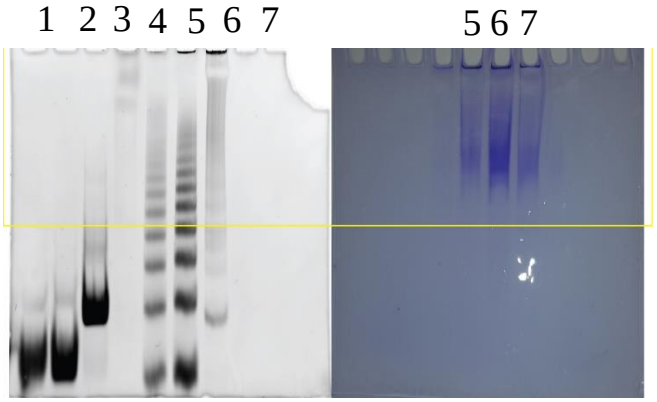

Legend
1. Sense
2. Antisense
3. Sense-Antisense Duplex
4. Unlabeled actin
5. actin-Sense
6. actin-Antisense
7. actin-S-AS-actin Duplex

Figure C. Gel Duplex Test

The Coomassie Blue gel indicated limited to no movement of unbound actin. This is due to a low overall charge of actin - which, at pH 8, is around -7 and may cause very little movement in the gel. DNA functionalized actin would have more mobility due to the electrophoretic movement caused by the more negatively charged DNA molecule attached, ergo, unlabeled actin does not travel through the gel while labeled actin does. The presence of the multilevel bands in

the EtBr gel indicated some proof of DNA-actin functionalization as well as Sense-AS duplex formation. The aggregation that is shown in both the Coomassie blue stain and the EtBr stain indicate aggregation of the functionalized actin at the top of the well. The presence of bands there in both gels points towards both DNA and actin being present